



**TABLE 1** Range of OTU similarity thresholds currently used in the literature for nitrogen-cycling genes to construct OTUs

| Gene  | Primer pair             | Reference(s) reporting similarity threshold of: |            |     |        |     |     |
|---|-------------------------|---|------------|-----|--------|-----|-----|
|   |                         | 97%   | 95%        | 90% | 85%    | 83% | 82% |
| AOB <i>amoA</i> (bacterial ammonia monooxygenase) | BacamoA-1F/BacamoA-2R   | 7, 8, 72–76                                     | 77–79      | 80  | 81, 82 |     |     |
| AOA <i>amoA</i> (archaeal ammonia monooxygenase)  | Arch-amoWAF/Arch-amoWAR | 7, 8, 73, 74, 76, 83, 84                        | 77, 79, 81 | 85  | 80–82  |     |     |
| <i>nirK</i> (nitrate reductase)                   | nirKFlaCu/nirKR3Cu      | 86–88   | 79         | 89  |        | 90  |     |
| <i>nirS</i> (nitrate reductase)                   | nirS1F/nirS3R           | 87, 88  | 91         | 89  |        |     | 90  |
| <i>nrfA</i> (nitrate reductase to ammonia)        | nrfAF2aw/nrfAR1         | 92  |            |     |        |     |     |
| <i>nxB</i> (nitrite oxidase)                      | nxB169f/nxB638r         | 93  |            |     |        |     |     |

in cell division and maintenance (housekeeping genes) can be used as an alternative to the *16S rRNA* gene for diversity estimation (3, 4) to circumvent the issue of intragenomic variation in the *16S rRNA* gene (5). Biogeochemical cycles can also be targeted via key functional genes involved in the processes of interest, e.g., the nitrogen cycle (6–11), the sulfur cycle (12, 13), and the methane cycle (14). The same is true for bioremediation (15, 16) and antibiotic resistance (17), to mention but a few possibilities. By targeting functional genes, we can start to unravel the functional potential of microbial communities, and if transcripts are targeted, actively transcribing organisms are revealed, a step closer to identifying the organisms driving the target processes.

Irrespective of the gene target, before hypothesis testing and ecological meaning can be inferred from amplicon data sets, the sequences first have to be grouped into taxonomically meaningful “units” to allow downstream analysis. There are two approaches for grouping amplicon data for downstream analysis: operational taxonomic units (OTUs) and amplicon sequence variants (ASVs). OTUs group sequences into a consensus sequence (the OTU) at a defined sequence similarity threshold. For the *16S rRNA* gene, a threshold of 97% sequence identity is generally used to define OTUs to the species level, although this value has been challenged (18). As functional genes may have been subject to significant horizontal gene transfer and may be present in poly- or monophyletic groups, the relationship between percent identity and taxonomic delimitation is not clear and is often unknown. As a result, in the literature, different similarity thresholds have been used to construct OTUs for the same functional gene target (Table 1), with an OTU at a threshold of 97% sequence identity (OTU-97%) being widely used, often without a clear rationale. This variation in OTU selection criteria makes it difficult to select a meaningful value and creates limitations when comparing data among studies. This is important as uncertainties in selecting the appropriate taxonomic cutoff could lead to different interpretations of findings underpinning our understanding of larger-scale ecological processes and mechanisms structuring microbial communities and their activities (19). For the *16S rRNA* gene, the choice of OTU similarity threshold used can significantly influence microbial diversity patterns (20, 21), and we hypothesize that this is also true for functional genes. In fact, some authors suggested that OTU similarity thresholds should be adjusted depending on the clustering algorithm and data complexity when phylogenetically divergent groups are present within the same community. This is because a single threshold for species delimitation is often not relevant due to the variable evolutionary rates of the *16S rRNA* gene across lineages (22, 23). Indeed, the use of strict thresholds has been shown to result in phylogenetically inconsistent (para- or polyphyletic) OTUs (24, 25).

After selection of the sequence similarity threshold, further choices need to be made. OTU clustering can be done using a closed-reference approach (22, 26) or by *de novo* assembly (22, 26). With the latter method, reads are clustered into OTUs without comparison to a preexisting database. This helps with the discovery of novel OTUs that are dissimilar to known sequences. However, the absence of comparison to known references makes *de novo* OTUs dataset-dependent, meaning that *de novo* OTUs from two different studies cannot be directly compared. On the other hand, the former approach makes it easier to compare OTUs between studies but limits the possibilities of discovering new sequences (26). The open-reference OTU-picking method combines the closed-reference

and *de novo* methods: reads are clustered against a reference database, and those that do not match reference sequences are clustered *de novo*. Even though this seems a good compromise between closed-reference and *de novo* methods, problems such as inflated richness and exaggerated between-sample diversity can still occur (27).

With the ASV approach (26), an error model is generated for the sequencing run, and reads are clustered in order to map this error model. The two most commonly used pipelines for ASV reconstruction are DADA2 (28), in which both forward and reverse reads are denoised and merged, and Deblur (29), in which forward reads can be used on their own to reconstruct ASVs. This is advantageous when amplicons are too long to be merged properly or when the quality of the reverse reads is poor (30). The ASV approach is appealing as it no longer groups amplicons based on a consensus sequence but instead resolves sequences with as little as a single nucleotide variation. Consequently, the ASV method does not require reference databases and is able to detect new sequences, and ASVs from different data sets can be directly compared (26). The ASV method has been compared to the OTU approach using phylogenetic markers (the 16S rRNA gene, the 18S rRNA gene, and the fungal internal transcribed spacer [ITS] region), and overall, the results indicate better accuracy (31–33) and sensitivity (34) of the former when tested against mock communities. The impact that this has on large-scale ecological patterns still needs to be fully understood as some research suggests that the biological conclusions drawn using either method, based on phylogenetic markers, are largely consistent (32, 35), while others suggest that HTS processing method (OTU versus ASV) can affect the interpretation of differentially abundant taxa between treatments (36). Nonetheless, as the use of ASVs does not rely on a user-defined threshold that may not hold biological meaning, this approach should increase the phylogenetic resolution of functional genes and, importantly, facilitate comparison of data among studies, as they should be able to segregate sequences on as little as one nucleotide variant. Consequently, ASVs are a promising approach for functional gene amplicon studies (13). However, how the use of ASVs versus OTUs impacts ecological interpretations based on functional genes is unclear.

After selecting the appropriate amplicon reconstruction method (ASVs or OTUs), the next immediate challenge is assigning taxonomy by matching against a reference database. For the 16S rRNA gene, several curated databases are available (e.g., Silva, GreenGenes, and Midas) and are routinely used. For most functional genes, no such databases are available, and the reference sequences used to assign taxonomy often vary among studies. The most popular approaches for assigning taxonomy rely on the pattern recognition of overlapping “words” of length  $k$  (generally  $k = 8$ ), called  $k$ -mers. The frequency of matching  $k$ -mers between the query and reference sequences is used as a measure of sequence similarity: a higher frequency of shared  $k$ -mers indicates higher similarity between the query and reference sequences. This approach is fast, objective, and not limited by the uncertainties associated with methods based on evolutionary models and alignments (37, 38). This approach is usually implemented as a classifier, such as the commonly used naive Bayesian classifier (NBC). One main limitation of this approach is that it uses the assumption that the actual position of the  $k$ -mers in the sequence is not important, whereas in reality, two sequences with the same  $k$ -mers but in different orders are different. Furthermore, the optimal choice of length for the  $k$ -mer might vary depending on the target gene or the region within the same gene (39). Another approach is the Bayesian lowest common ancestor (BLCA) algorithm (39), where the query sequence is subjected to a BLAST search against a reference database(s) and significant “hits” are recorded. The taxonomy of the query sequence is assigned as the lowest common ancestor between these hits. For example, if a query sequence has significant matches to two *Nitrosomonas europaea* reference sequences, the query sequence will be assigned to the species *Nitrosomonas europaea* as it is the lowest common ancestor between the two hits. However, if a query sequence has two different hits, *Nitrosomonas europaea* and *Nitrosomonas oligotropha*, the query sequence will be assigned to the genus *Nitrosomonas*. By considering hit results from multiple databases, the BLCA approach is able to provide probabilistic-based confidence values at each taxonomic level of this assignment. Previously, the BLCA method was shown to provide better species-level resolution than the NBC for 16S rRNA gene sequences (39, 40). How they compare for functional genes has yet to be determined.

The aim of this study is to compare the effects of amplicon reconstruction approaches, OTUs (at a range of sequence similarity values) versus ASVs, and taxonomic assignment methods, NBC versus BLCA, on a suite of functional genes. We do this to determine if diversity measures and subsequent ecological interpretations are affected by these choices. We hypothesize that both alpha and beta diversity measures will differ depending on the amplicon-processing methods used. To do this, we examine the nitrogen cycle in marine sediments of Marennes-Oléron Bay on the French Atlantic coast. The middle part of the bay, the Brouage mudflat, is characterized by the presence of flow-parallel sediment structures consisting of crests (ridges) and troughs (runnels). These side-by-side physical structures have been shown to significantly affect the nitrification rates (higher in runnels) (41, 42). We ask if the physical structure of the ridges and runnels results in differences in the diversity of the nitrogen-cycling community present. Different pathways of the nitrogen cycle are targeted via genes encoding key enzymes. Specifically, nitrification, the oxidation of ammonia to nitrate via nitrite, is targeted via subunit A of ammonia monooxygenase (*amoA*) and the beta subunit of nitrite oxidoreductase (*nxrB*); denitrification, the sequential reduction of nitrate to dinitrogen gas, is targeted via the nitrite reductase genes *nirS* and *nirK*; and dissimilatory nitrate reduction to ammonia (DNRA) is targeted via the cytochrome *c* nitrite reductase gene *nrfA*.

## RESULTS

**Conversion of raw reads to OTUs/ASVs.** For all genes except *nrfA* and *amoA* from ammonia-oxidizing archaea (AOA *amoA*), there was a high percentage (~70% to ~95%) of reads converted from raw reads to OTUs/ASVs. The use of OTUs generally resulted in a higher percentage of reads being retained for *amoA* from ammonia-oxidizing bacteria (AOB *amoA*) (80.57% to 84.74%) than the use of ASVs (79.61%). An opposite trend was observed for *nxrB* (87.03% for ASVs versus 77.55% for OTUs), *nirK* (95.33% for ASVs versus 86.41% to 93.45% for OTUs), and *nirS* (90.92% for ASVs versus 77.76% to 78.98% for OTUs). For AOA *amoA* and *nrfA*, low percentages of reads were retained when using OTUs (32.86% for *nrfA* and 14.50% to 30.26% for AOA *amoA*), whereas the ASV method allowed a good conversion of raw reads (62.75% for *nrfA* and 94.43% for AOA *amoA*) (Table 2).

**OTU/ASV quality check.** A quality check based on translated OTU/ASV sequences was performed to ensure that only high-quality reads were retained for downstream analyses. First, amino acid (AA) sequences containing stop codons were deleted. Next, AA sequences were sorted depending on their sizes. Those shorter or longer than the expected size were subjected to a BLAST analysis using BLASTp and were retained only if they matched the expected enzyme (Fig. 1). A high number of sequences were found to either contain stop codons or not translate to the correct protein (e.g., for AOB *amoA*, 57.8% to 94.70% of the sequences did not pass the quality-filtering step). For all genes tested, even though the absolute number of error-prone sequences increased, their proportion decreased when using ASVs compared to OTUs and increased as the percent similarity decreased for OTU construction (Table 2). These error-prone sequences, despite being numerous, represented only a small fraction of the total abundance. Indeed, between ~90% and ~99% of the reads that passed the processing steps were retained after the quality-filtering step.

As shown in Fig. S1 in the supplemental material, there was an overlap between the sizes of the correct and error-prone AA sequences. A simple gating system based on protein size could therefore not be used to automatically remove the error-prone sequences. A manual check based on a BLAST analysis of AA sequences that are shorter or longer than the expected length therefore remains the best option for verification. The only exception was for AOB *amoA* when using ASVs, where only the AA sequences with exactly the expected length were found to be correct proteins.

**Effects of OTU thresholds and ASV selection on alpha diversity and sequence coverage. (i) Alpha diversity indices.** Richness, Simpson, and Shannon indices were calculated based on the rarefied abundance tables. To allow comparison between amplicon-processing methods, abundance tables were rarefied to 10,000 reads. Samples that contained fewer than 10,000 reads were not included in the analysis. In general, an increase in the percent identity used to generate OTUs resulted in an increase in the values of alpha diversity indices

**TABLE 2** Read loss during the processing of HTS data using OTU and ASV pipelines

| Gene and pipeline | No. of reads for OTU/ASV processing <sup>a</sup> |                   |            |           | Quality filtering (AA sequences) |                             |                  |                       |             |                   |                   |                               |
|-------------------|--|-------------------|------------|-----------|----------------------------------|-----------------------------|------------------|-----------------------|-------------|-------------------|-------------------|-------------------------------|
|                   | Raw reads  | Quality filtering | Correction | Merging   | Chimeras                         | Final conversion to ASV/OTU | Unique ASVs/OTUs | No. of filtered reads | % raw reads | % processed reads | % wrong ASVs/OTUs | Final no. of unique ASVs/OTUs |
| AOB amoA          |  |                   |            |           |                                  |                             |                  |                       |             |                   |                   |                               |
| ASV               | 1,086,576  | 1,086,576         | NA         | 993,017   | 98,787                           | 894,230                     | 910              | 864,996               | 79.61       | 96.73             | 57.80             | 384                           |
| OTU-97%           | 1,086,576  | 1,084,818         | 1,084,051  | 1,072,646 | 12,620                           | 907,973                     | 274              | 875,443               | 80.57       | 96.42             | 79.20             | 57                            |
| OTU-95%           | 1,086,576  |                   |            |           | 6,565                            | 938,258                     | 205              | 895,785               | 82.44       | 95.47             | 83.90             | 33                            |
| OTU-90%           | 1,086,576  |                   |            |           | 22                               | 974,070                     | 166              | 910,044               | 83.75       | 93.43             | 90.96             | 15                            |
| OTU-85%           | 1,086,576  |                   |            |           | 2                                | 994,878                     | 151              | 920,739               | 84.74       | 92.55             | 94.70             | 8                             |
| AOA amoA          |  |                   |            |           |                                  |                             |                  |                       |             |                   |                   |                               |
| ASV               | 1,714,971  | 1,713,630         | NA         | 1,660,869 | 36,563                           | 1,624,306                   | 596              | 1,619,524             | 94.43       | 99.71             | 4.53              | 569                           |
| OTU-97%           | 1,714,971  | 1,707,358         | 1,705,368  | 591,774   | 7                                | 251,981                     | 137              | 248,737               | 14.50       | 98.71             | 18.98             | 111                           |
| OTU-95%           | 1,714,971  |                   |            |           | 0                                | 322,959                     | 64               | 314,603               | 18.34       | 97.41             | 21.88             | 50                            |
| OTU-90%           | 1,714,971  |                   |            |           | 28                               | 414,551                     | 21               | 410,824               | 23.96       | 99.10             | 28.57             | 15                            |
| OTU-85%           | 1,714,971  |                   |            |           | 0                                | 522,952                     | 12               | 518,934               | 30.26       | 99.23             | 50.00             | 6                             |
| nrxB              |  |                   |            |           |                                  |                             |                  |                       |             |                   |                   |                               |
| ASV               | 297,508  | 297,404           | NA         | 285,919   | 24,575                           | 285,919                     | 861              | 258,935               | 87.03       | 90.56             | 5.23              | 816                           |
| OTU-97%           | 297,508  | 297,295           | 296,968    | 296,494   | 146                              | 249,994                     | 372              | 230,712               | 77.55       | 92.29             | 10.48             | 333                           |
| nirK              |  |                   |            |           |                                  |                             |                  |                       |             |                   |                   |                               |
| ASV               | 1,317,256  | 1,316,137         | NA         | 1,274,893 | 7,957                            | 1,266,936                   | 2,331            | 1,258,340             | 95.53       | 99.32             | 2.27              | 2,278                         |
| OTU-97%           | 1,317,256  | 1,305,520         | 1,302,639  | 1,150,918 | 1,842                            | 1,169,122                   | 1,074            | 1,138,188             | 86.41       | 97.35             | 5.77              | 1,012                         |
| OTU-95%           | 1,317,256  |                   |            |           | 1,693                            | 1,192,377                   | 918              | 1,178,126             | 89.44       | 98.80             | 5.01              | 872                           |
| OTU-90%           | 1,317,256  |                   |            |           | 62                               | 1,215,020                   | 701              | 1,210,577             | 91.90       | 99.63             | 5.42              | 663                           |
| OTU-83%           | 1,317,256  |                   |            |           | 2                                | 1,235,483                   | 330              | 1,230,920             | 93.45       | 99.63             | 10.30             | 296                           |
| nirS              |  |                   |            |           |                                  |                             |                  |                       |             |                   |                   |                               |
| ASV               | 1,410,146  | 1,409,380         | NA         | 1,326,808 | 42,336                           | 1,284,472                   | 2,190            | 1,282,047             | 90.92       | 99.81             | 5.57              | 2,068                         |
| OTU-97%           | 1,410,146  | 1,404,968         | 1,404,097  | 1,215,878 | 42                               | 967,658                     | 248              | 960,374               | 68.10       | 99.25             | 15.32             | 210                           |
| OTU-95%           | 1,410,146  |                   |            |           | 169                              | 1,052,876                   | 204              | 1,045,334             | 74.13       | 99.28             | 14.71             | 174                           |
| OTU-90%           | 1,410,146  |                   |            |           | 0                                | 1,124,335                   | 155              | 1,113,700             | 78.98       | 99.05             | 14.19             | 133                           |
| OTU-82%           | 1,410,146  |                   |            |           | 0                                | 1,124,622                   | 63               | 1,096,597             | 77.76       | 97.51             | 25.40             | 47                            |
| nirA              |  |                   |            |           |                                  |                             |                  |                       |             |                   |                   |                               |
| ASV               | 1,829,948  | 1,829,295         | NA         | 1,603,920 | 444,687                          | 1,159,233                   | 7,520            | 1,148,346             | 62.75       | 99.06             | 1.41              | 7,414                         |
| OTU-97%           | 1,829,948  | 1,829,382         | 1,828,735  | 1,219,228 | 8                                | 614,215                     | 117              | 601,388               | 32.86       | 97.91             | 11.97             | 103                           |

<sup>a</sup>NA, not applicable.

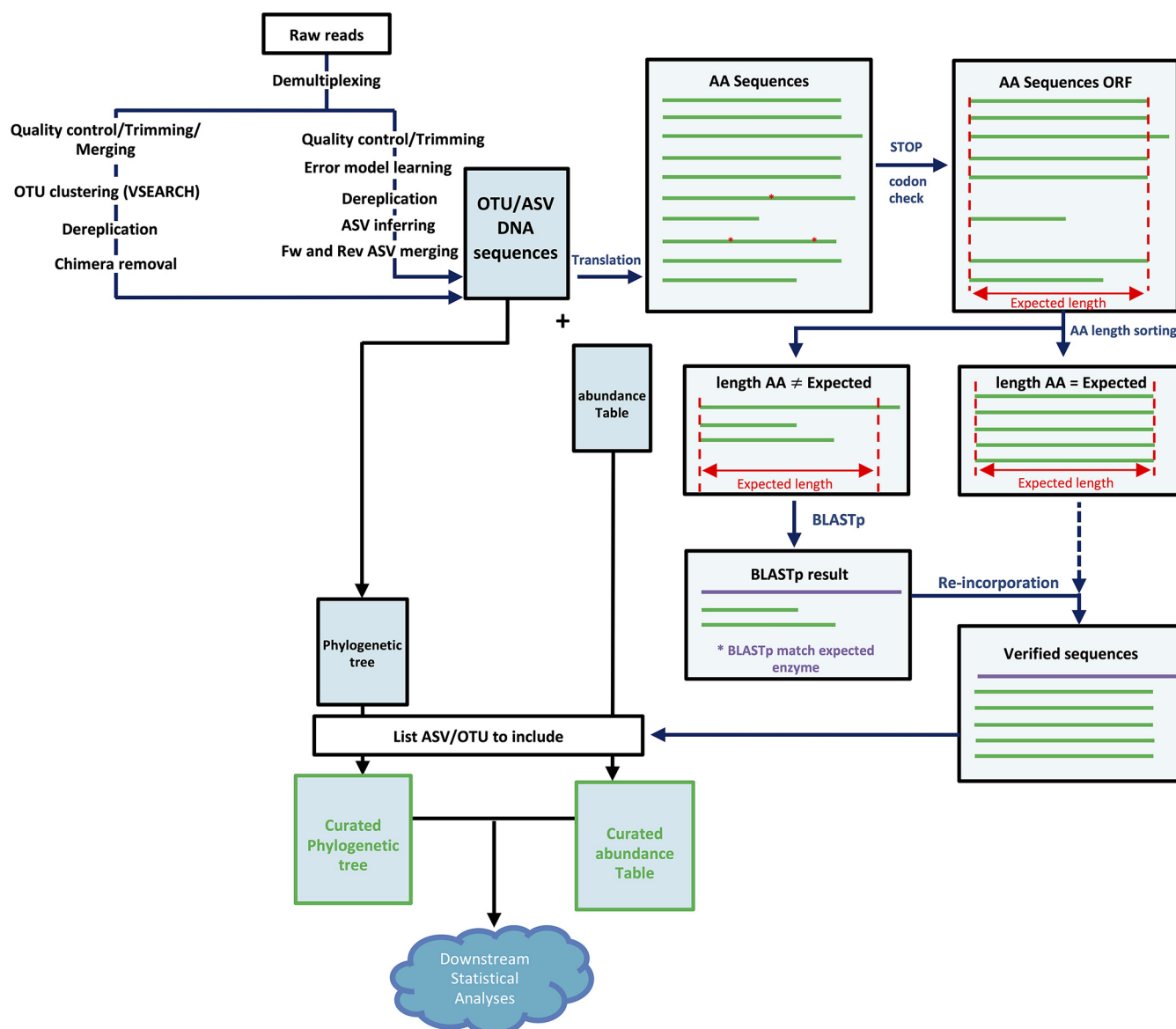


**FIG 1** OTU/ASV quality check workflow (example of the bacterial *amoA* gene). Red asterisks indicate stop codons. Fw, forward; Rev, reverse; ORF, open reading frame.

(Fig. 2). A similar increase was generally observed when using ASVs instead of OTUs. The increases in alpha diversity indices between OTUs and ASVs were particularly strong for *nirS* and *nrfA* (all indices) and AOB *amoA* (richness). For AOA *amoA*, there were slight decreases in Shannon and Simpson indices from OTU-97% to ASVs for runnel samples. Interestingly, the use of OTUs (97%) and ASVs could lead to different interpretations as to which of the two sedimentary structures was the most diverse. When using OTU-97%, ridges had higher Shannon ( $P < 0.05$ ) and Simpson ( $0.01 < P < 0.05$ ) index values than runnels, and the inverse was found when using ASVs ( $0.01 < P < 0.05$  for Shannon and  $P < 0.001$  for Simpson). A similar trend was observed for *nrfA*, with higher richness ( $0.01 < P < 0.05$ ), Shannon ( $P < 0.001$ ), and Simpson ( $0.01 < P < 0.05$ ) values in ridges than in runnels when using OTU-97% and higher richness ( $P < 0.05$ ), Shannon ( $P < 0.05$ ), and Simpson ( $P < 0.05$ ) values in runnels when using ASVs (Fig. 2) (Table S4).

**(ii) Rarefaction curves.** To determine if the sequencing effort had been sufficient to capture the full OTU/ASV diversity, rarefaction curves were drawn for all genes using the OTU and ASV abundance tables. When sequencing reads were clustered using the OTU approach, the rarefaction curves generally reached a quasiplateau phase,



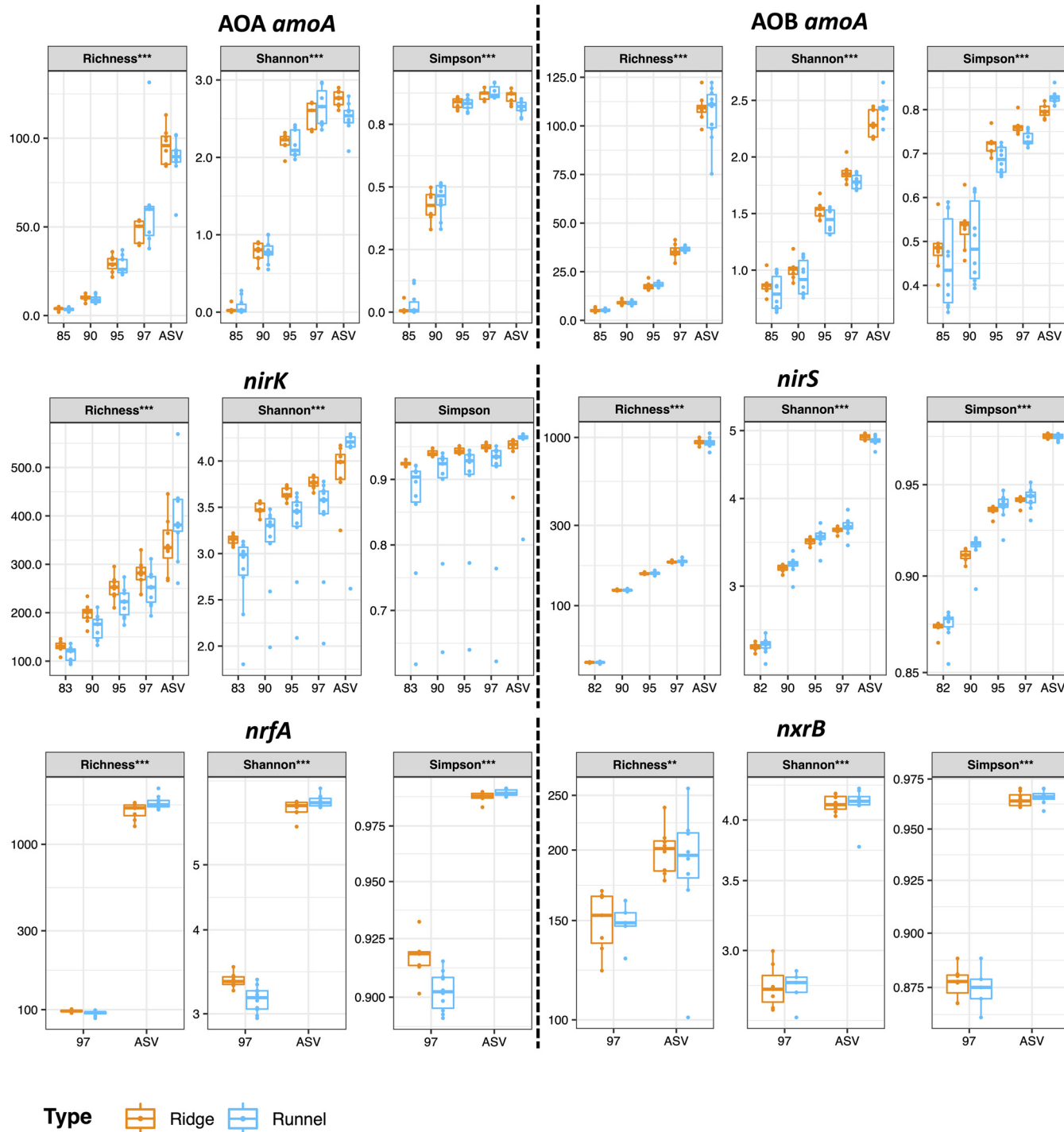


**FIG 2** Effects of different OTU sequence similarity thresholds versus ASVs on alpha diversity results. Results of analysis of variance (ANOVA) for the effect of the clustering method on richness, Simpson, and Shannon indices are reported at the top of each plot for each gene. \*,  $P < 0.05$ ; \*\*,  $0.01 > P > 0.001$ ; \*\*\*,  $P < 0.001$ .

indicating that the observed richness was close to its maximum theoretical value. For *nirK* and *nrxB*, this plateau phase was not reached, indicating that more OTUs would have been recovered with greater sequencing depth. Rarefaction curves obtained from ASV abundance tables were generally farther from reaching the plateau than curves obtained using the OTU approach (Fig. 3).

**Effect of OTU thresholds and ASVs on beta diversity. (i) Dissimilarity distances between samples.** To determine the effect of the amplicon data analysis method on

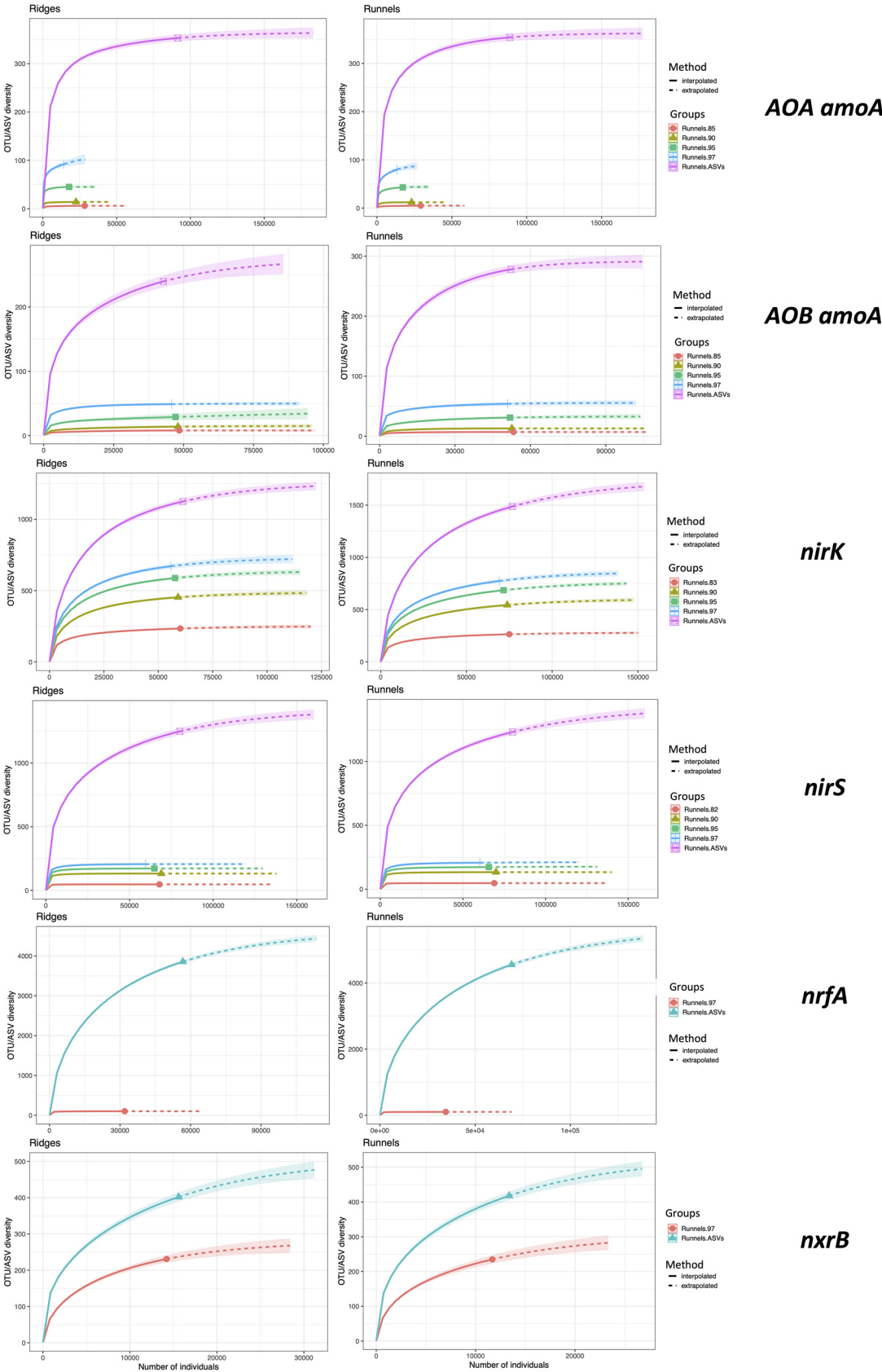


**FIG 3** Rarefaction curves in ridges and runnels using different OTU sequence similarity thresholds and ASVs.



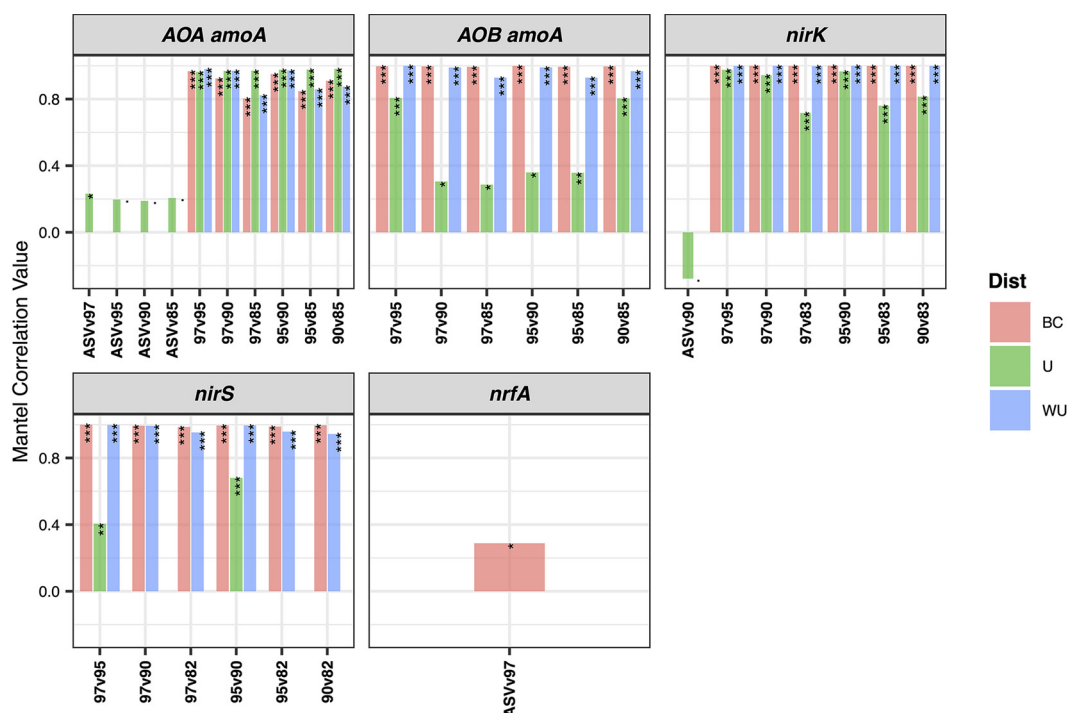


**FIG 4** Effects of different OTU sequence similarity thresholds or ASV amplicon reconstruction approaches on phylogenetic distances. Distance matrices were calculated using Bray-Curtis (BC), UniFrac (U), and weighted UniFrac (WU) metrics at different OTU similarity thresholds and ASVs for each gene. Pairwise correlations between matrices, as indicated on the x axis, were calculated using a Mantel test. The *P* values of the tests are reported at the top of the bar plots. ·,  $0.05 < P < 0.1$ ; \*,  $P < 0.05$ ; \*\*,  $0.01 > P > 0.001$ ; \*\*\*,  $P < 0.001$ .

the dissimilarity distance between samples, Mantel correlations were calculated among distance matrices obtained using Bray-Curtis (BC), UniFrac (U), and weighted UniFrac (WUniFrac) metrics. A strong effect of the approach used is seen, as reflected by Mantel correlations different from a value of 1. For all genes tested, low correlations between distance matrices obtained with ASVs versus OTUs were observed ( $\sim 0.2$  or lower [ $P > 0.5$ ]). In contrast, the correlations between distance matrices obtained with OTUs at different similarity thresholds were generally high ( $> 0.8$  [ $P < 0.01$ ]), except for the UniFrac distance matrices for AOB *amoA* and *nirS*, where lower correlation values were generally observed (Fig. 4).

**(ii) Differences in communities between ridges and runnels.** To determine whether the method used to process sequencing reads could significantly affect the beta diversity results, Bray-Curtis, UniFrac, and WUniFrac distances between communities in the two sedimentary structures (ridges and runnels) were calculated, and their significance was tested using permutational multivariate analysis of variance (PERMANOVA). The effect of the clustering method was different depending on the gene of interest (Fig. 5). For AOA *amoA*, significant differences in WUniFrac distances between ridges and runnels were seen when reads were clustered using the ASVs or OTUs at 97% and 85% similarity thresholds but not when using OTUs at 95% and 90% similarity thresholds. For *nirS*, significant differences were observed for WUniFrac when using ASVs, OTU-82%, and OTU-90% but not when using OTU-95% and OTU-97%. When considering UniFrac distances, significant differences were observed for *nrfA* and *nirS* communities when using ASVs but not when using OTU-97%, and the inverse was found for AOB *amoA*. For *nirK* and *nxB*, the different clustering methods were more consistent, with no significant effect of the data analysis pipeline on beta diversity (Fig. 5). To summarize, the clustering method used for amplicons had a significant effect on beta diversity for some genes, while other were less affected.

To better understand the effect of the HTS data processing method on the phylogeny of representative sequences, phylogenetic trees were drawn using representative OTUs/ASVs along with full-length or quasi-full-length sequences downloaded from the NCBI or Fungene

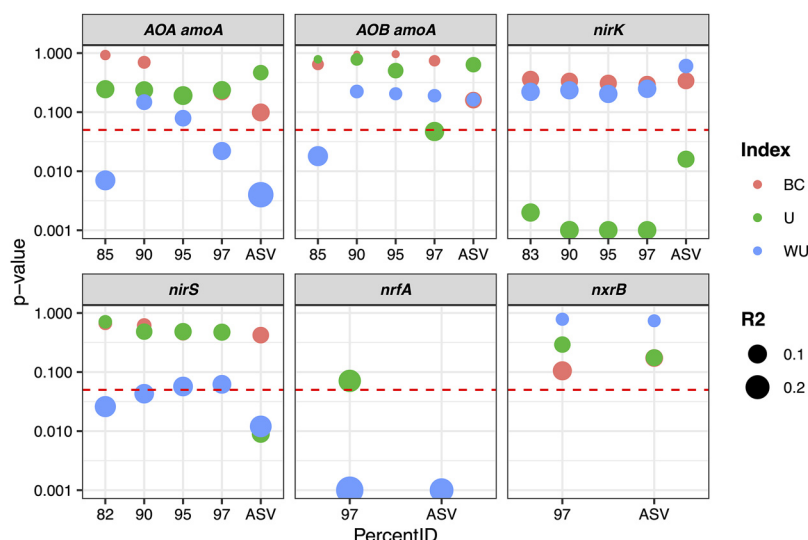


**FIG 5** Effect of the amplicon reconstruction method on beta diversity results. The reported  $P$  values show the effect of the ridge/runnel structure on the community composition determined by the sequencing of six different nitrogen cycle genes using three different dissimilarity distances, indicated by the color of the symbols, as explained in the key. The horizontal dashed red line represents the  $P$  value threshold for significance (0.05). The size of the points represents the  $R^2$  value, i.e., the percentage of variance in the Bray-Curtis (BC), UniFrac (U), and weighted UniFrac (WU) metrics explained by the ridge/runnel structures.

database. Tree dissimilarities increased as the number of representative sequences in the trees increased following natural logarithm regression [Robinson-Foulds distances,  $RF.distance = a \times \ln(\text{number of sequences}) + b$ ], indicating a strong effect of the HTS data processing method on the phylogeny of representative sequences (Fig. S2).

**Effects of OTU thresholds and ASVs on canonical analyses.** Canonical analyses, e.g., canonical correspondence analysis (CCA), are useful approaches to analyze, detect, and visualize interactions between microbial communities and environmental parameters. CCA measures the association between an explanatory table (the physicochemical parameters) and a response table (the abundance table). Previously, it was shown that, in some cases, the amplicon reconstruction method affects the composition of the abundance tables, as revealed by Mantel correlations between Bray-Curtis distance matrices obtained from ASVs or OTUs at different similarity thresholds of  $<1$  (Fig. 4). These changes in the abundance tables can be expected to also change the results of CCA. To test this, CCA was done using the abundance tables obtained from the different amplicon reconstruction methods (range of OTU sequence similarity thresholds and ASVs) using the same physicochemical data table. As shown in Table 3, the choice of amplicon processing method strongly impacted the results, except for *nxrB*, where no significant drivers were found regardless of the method used.

For ammonia oxidizers, when using ASVs, chlorophyll *a* was a weak driver ( $0.1 < P < 0.05$ ) of AOB communities, and sediment grain size (SGS) was a significant driver of AOA. When using OTUs, ammonia and chlorophyll *a* became significant drivers of AOB at a 97% similarity threshold, while SGS became a significant driver for lower similarity thresholds. For AOA, pH and SGS were significant drivers at a 95% similarity threshold. SGS remained significant at 90%, while pH did not.

For the nitrite-oxidizing community, again, differences were seen depending on the amplicon reconstruction approach. Total organic carbon (TOC) was found to be a driver for *nirK*, except for OTU-90%, while SGS was a significant driver only when using OTU-97% and OTU-83%. For *nirS*, ammonia was a strong driver ( $P < 0.01$ ) only when using ASVs. Total dissolved nitrogen (TDN) and chlorophyll *a* were significant drivers only when using ASVs and OTU-82%, respectively. For *nrfA*, ammonia was also a strong driver ( $P < 0.01$ ) only when using ASVs, while nitrate and chlorophyll *a* were significant when using OTU-97%.

**NBC versus BLCA for taxonomic classification.** For the majority of genes studied here, neither the NBC nor the BLCA method performed well, with the majority of ASVs

**TABLE 3** Canonical correspondence analysis<sup>a</sup>

| Pipeline        | Significance    |                              |                              |      |    |     |     |     |     |
|-----------------|-----------------|------------------------------|------------------------------|------|----|-----|-----|-----|-----|
|                 | NH <sub>3</sub> | NO <sub>2</sub> <sup>-</sup> | NO <sub>3</sub> <sup>-</sup> | ChlA | pH | SGS | TOC | DOC | TDN |
| AOB ASV         |                 |                              |                              | .    |    |     |     |     |     |
| AOB 97          |                 |                              |                              |      | .  | .   |     |     |     |
| AOB 95          |                 |                              | .                            | .    | *  | *   |     |     |     |
| AOB 90          |                 |                              |                              |      |    | *   |     |     |     |
| AOB 85          |                 |                              |                              |      |    | .   |     |     |     |
| AOA ASV         |                 |                              |                              |      |    | *   |     |     |     |
| AOA 97          | *               |                              |                              | *    |    |     |     |     |     |
| AOA 95          |                 |                              |                              |      |    | *   |     |     |     |
| AOA 90          |                 |                              |                              |      |    | **  |     |     |     |
| AOA 85          |                 |                              |                              |      |    | *   |     |     |     |
| <i>nirK</i> ASV |                 |                              |                              |      |    |     | *   |     |     |
| <i>nirK</i> 97  |                 |                              |                              |      |    | *   | *   |     |     |
| <i>nirK</i> 95  |                 |                              |                              |      |    | .   | *   |     |     |
| <i>nirK</i> 90  |                 |                              |                              |      |    |     | .   |     |     |
| <i>nirK</i> 83  |                 |                              | .                            |      |    | **  | **  | .   |     |
| <i>nirS</i> ASV | ***             |                              |                              |      |    |     |     |     | *   |
| <i>nirS</i> 97  |                 |                              |                              |      |    |     |     |     |     |
| <i>nirS</i> 95  |                 |                              |                              |      |    |     |     |     |     |
| <i>nirS</i> 90  |                 |                              |                              | .    |    |     |     |     |     |
| <i>nirS</i> 82  |                 |                              |                              | *    |    |     |     |     |     |
| <i>nxrB</i> ASV |                 |                              |                              |      |    |     |     |     |     |
| <i>nxrB</i> 97  |                 |                              |                              |      |    |     |     |     |     |
| <i>nrfA</i> ASV | ***             |                              |                              |      |    |     |     |     |     |
| <i>nrfA</i> 97  | .               |                              | *                            | *    | .  |     |     |     |     |

<sup>a</sup>Empty cells indicate that the physicochemical parameter is not a driver of the community. ., 0.1 > *P* > 0.05; \*, *P* < 0.05; \*\*, 0.01 > *P* > 0.001; \*\*\*, *P* < 0.001. ChlA, chlorophyll *a*; SGS, sediment grain size (percent <63 μm); TOC, total organic carbon; DOC, dissolved organic carbon; TDN, total dissolved nitrogen; Pipeline' indicates the target gene and the HTS method. e.g. AOB 97, AOB OTU at a threshold of 97% sequence identity.

being unassigned at the species level when using the Fungene database. This is likely an indication of the lack of environmental sequences with species-level-defined taxonomy in this database. The only exception was for *nrfA*, with the NBC approach resulting in only 17.27% of ASVs being unassigned, versus the BLCA method, in which 100% were unassigned. Both NBC and BLCA performed better when a custom database was used to assign taxonomy (AOA and AOB *amoA*). In this case, BLCA performed slightly better than NBC for AOA *amoA*, with 72.89% and 90.85% of ASVs being unassigned with BLCA and NBC, respectively. Inversely, for AOB *amoA*, NBC performed slightly better than BLCA, with 0.01% and 6.68% of ASVs being unassigned with NBC and BLCA, respectively (Table 4). To determine what caused these differences for AOB *amoA*, a phylogenetic tree was constructed with AOB *amoA* ASVs and sequences from known AOB isolates downloaded from the NCBI database. The main differences in the taxonomic assignments for AOB *amoA* ASVs were for some sequences assigned as *Nitrosomonas aestuarii* with NBC that were unassigned using BLCA (Fig. 6).

## DISCUSSION

The aim of this study was to evaluate the effect of the selection of different OTU similarity thresholds versus the ASV approach for amplicon sequence data processing. This was tested using a suite of functional genes targeting different pathways of the nitrogen cycle. We determined the effect that these choices had on alpha and beta diversity values and subsequent CCA. We also examined the effect of the approach taken for the taxonomic assignment of functional genes using the nitrogen cycle communities from ridges and runnels of the Montportail-Brouage mudflat as a case study.

**TABLE 4** Performances of the NBC and BLCA methods for taxonomic assignment (ASVs)

| Target          | Taxonomic method | Database | % unassigned species |
|-----------------|------------------|----------|----------------------|
| AOB <i>amoA</i> | NBC              | Fungene  | 100                  |
|                 |                  | Custom   | 0.01                 |
|                 | BLCA             | Fungene  | 100                  |
|                 |                  | Custom   | 6.68                 |
| AOA <i>amoA</i> | NBC              | Fungene  | 84.72                |
|                 |                  | Custom   | 90.85                |
|                 | BLCA             | Fungene  | 100                  |
|                 |                  | Custom   | 72.89                |
| <i>nxrB</i>     | NBC              | Fungene  | 78.92                |
|                 | BLCA             |          | 60.02                |
| <i>nirK</i>     | NBC              | Fungene  | 99.91                |
|                 | BLCA             |          | 99.95                |
| <i>nirS</i>     | NBC              | Fungene  | 100                  |
|                 | BLCA             |          | 100                  |
| <i>nrfA</i>     | NBC              | Fungene  | 17.27                |
|                 | BLCA             |          | 100                  |

The choice of amplicon reconstruction method had a significant effect on biological observations (Fig. 2, 4, and 5). As a result, the conclusions of this study based on OTUs (with different similarity thresholds) or ASVs lead to different ecological conclusions. Indeed, when comparing WUniFrac distances using the ASV denoising approach, we conclude that there was a significant effect of the ridge/runnel sedimentary structures on AOA *amoA*, *nirS*, and *nrfA*. On the other hand, we conclude that there was a non-significant effect on AOA *amoA* with OTU-95% and OTU-90% and *nirS* with OTU-97% and OTU-95%. For AOB *amoA*, using the ASV method, we conclude that there was a nonsignificant effect of the ridge/runnel structures and a significant effect with OTU-85% (WUniFrac distances) and OTU-97% (UniFrac distances). To further understand the effect of the choice of ASVs versus OTUs on phylogenetic resolution, phylogenetic trees were constructed from ASVs and OTUs. For all target genes, an increase in dissimilarity was observed as the number of ASVs/OTUs compared increased, indicating that the choice of amplicon reconstruction method modifies the phylogeny of representative sequences (see Fig. S2 in the supplemental material).

The results from this study show the strong effect that the processing method has on the interpretation and biological understanding of sequencing data. This further illustrates the need for a standardized protocol for amplicon data processing to facilitate comparisons of data between studies. To date, there is no consensus as to which threshold to use to construct OTUs for the same gene amplified with the same primers (Table 1), and we therefore argue that ASVs, which do not require user-defined similarity thresholds, offer a better chance to achieve such standardization. The ASV method also generally resulted in a higher percentage of raw reads retained than with the OTU method, especially for AOA *amoA* and *nrfA*. Previous studies have shown that retaining more reads after amplicon processing improves the accuracy of microbiome analyses, especially for low-abundance species (43). This further strengthens our recommendation to use ASVs for functional gene HTS data processing. We further showed that the choice of amplicon reconstruction method affects the outcomes of multivariate analyses, which are routinely used to inform associations between biological assemblages and environmental parameters. For example, research on nitrification in the environment often seeks to determine the extent to which ammonia, pH, salinity, and temperature, etc., are significant drivers of the niche differentiation between AOA and AOB (7–9, 44–51). This study clearly

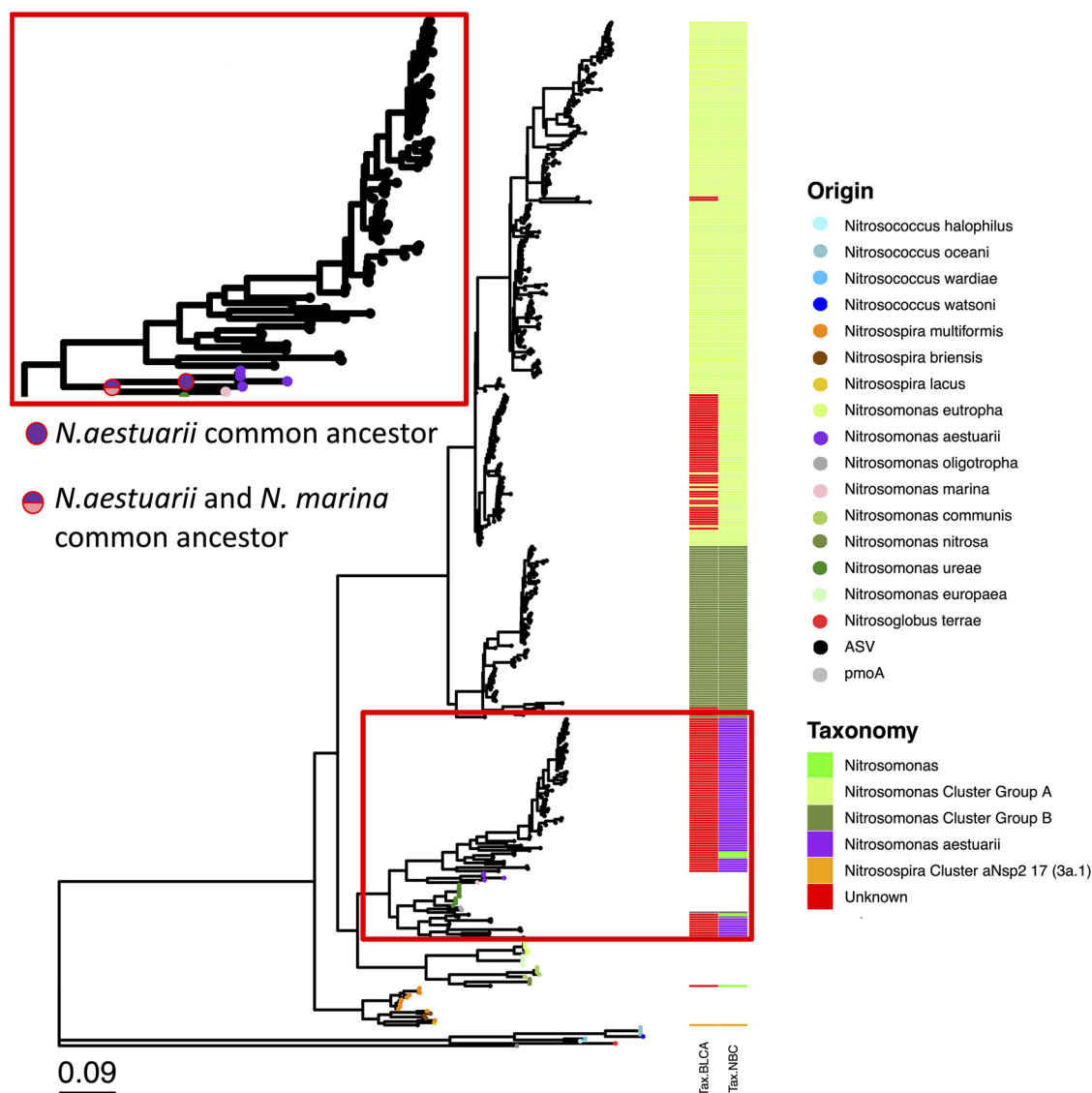


**FIG 6** NBC versus BLCA for the taxonomic assignment of AOB *amoA* ASVs. The taxonomy of representative sequences is indicated by the color of the tips on the tree. Taxonomy assigned by NBC (Tax.NBC) and BLCA (Tax.BLCA) for each ASV is represented at the right of the tree. The main point of disagreement between NBC and BLCA is shown by the red rectangle (see the zoomed-in view at the top left).

shows that the influence of environmental parameters on ammonia-oxidizing communities is dependent on the amplicon reconstruction method used. A consensus standardized method needs to be adopted in molecular microbial ecology to allow metareviews of current literature and the identification of ecological patterns that are not study-dependent (51, 52).

Other studies have reported that for *16S rRNA* gene amplicon sequencing, ecological patterns are robust to the choice of OTUs versus ASVs (32, 35, 52, 53). It could therefore be hypothesized that the difference between the *16S rRNA* gene as reported elsewhere and functional genes is due to a resolution effect: when targeting a high-diversity gene such as the *16S rRNA* gene by amplicon sequencing, we obtain an overall picture of the microbial community. Therefore, the use of OTUs (low resolution) or ASVs (high resolution) matters less because we still see the overall trends in the bacterial community. However, when investigating a phylogenetically tight group, we are already zoomed in on a small part of that microbial community, which explains why we need a higher resolution, i.e., ASVs, to differentiate each member of the community.

This study also provides a comparison between NBC and BLCA for the taxonomic assignment of functional gene sequences. We found that the BLCA method performed better

than the NBC for AOA *amoA* when using a custom database, and the inverse was found for AOB *amoA* due to some sequences being assigned to *Nitrosomonas aestuarii* when using NBC and being unassigned when using BLCA. When comparing these sequences to known representatives, it was observed that known AOB *amoA* sequences from *Nitrosomonas aestuarii* were clustered, and the common ancestor for all *N. aestuarii* strains did not include any of these ASVs. In fact, based on this tree, *N. aestuarii* and *Nitrosomonas marina* share an ancestor that does not include any ASV sequences. Based on this phylogeny, these ASVs could therefore not be members of the *N. aestuarii* group (Fig. 6). We conclude that for AOB *amoA*, the BLCA method, despite resulting in a lower number of sequences identified to the species level, resulted in a classification that made more sense from a phylogenetic point of view. This result is coherent with previous research showing the superiority of BLCA versus NBC for the taxonomic assignment of *16S rRNA* gene reads (40). However, the BLCA method performed much worse than NBC for the taxonomic assignment of *nrfA* sequences, with the vast majority (98.8%) being unassigned sequences, versus 18.8% with NBC. This likely reflects limitations in the database used rather than a problem with the BLCA method itself. Indeed, the majority of *nrfA* sequences in the Fungene database are full-length sequences originating from cultured microorganisms, which likely differ from sequences retrieved from the environment. To test this hypothesis, a phylogenetic tree was drawn using the top 200 *nrfA* ASVs found in this study and sequences from the reference database (covering 220 different genera). ASV sequences and representatives from the reference database generally formed separate clusters in the tree (Fig. S3). As a result, it can be expected that when ASVs are subjected to a BLAST search against the reference database, the significant matches do not share an ancestor at the genus level, and as a result, the BLCA algorithm cannot assign taxonomy at the genus or species level. In summary, the results from this study indicate that when the reference database is relevant to the sequences amplified (e.g., reference AOB *amoA* sequences from marine sediments to assign AOB *amoA* ASVs from marine sediments), the BLCA method is the best approach. On the other hand, if the reference database consists of sequences more dissimilar to the one retrieved from the environment, the NBC method might be more advisable to obtain taxonomic information, but the accuracy of this taxonomy might be low. ASVs have substantial merits for the analysis of functional genes for which OTU similarity values are unknown, and in general, the field is shifting to ASV-based resolution of amplicons (e.g., see reference 13). Yet the reference databases used to taxonomically place the amplicons are still based on traditional threshold-based clustering and should improve as more and more ASV-based studies become available in the future.

Currently, there is a shift in microbial ecology from OTUs to ASVs, and this approach has now been widely adopted for *16S rRNA* gene studies (33, 36, 54). The use of ASVs frees us from using similarity thresholds and produces relevant sequences that can be directly compared between studies; we suggest that it offers a pragmatic approach for the standardization of functional gene amplicon sequencing data sets. However, Schloss (53) recently showed that the use of ASVs for the *16S rRNA* gene can artificially split bacterial genomes as copies of the gene in a single genome typically do not share 100% similarity. Several functional genes are also present in more than one copy in a genome, and their sequences can be slightly different (55, 56). In this case, a similar split will take place, and genes from the same organism will be separated. Merging functional genes based on their amino acid (AA) sequence similarity could be an option to reduce the risk of such artificial splits while conserving the functional diversity within the data set. On the other hand, merging at the protein level might overshadow differences between species/strains where synonymous mutations have accumulated. Furthermore, the chance of generating identical protein sequences will increase as the length of the amplified region decreases. For short amplicons with low diversity, merging at the protein level might therefore result in several species being merged. Further work is needed to understand how functional diversity informs ecological processes.

**Conclusion.** Besides the obvious advantage of not relying on an arbitrary threshold, the ASV method reflects the sequence diversity of a given functional gene in the environment. This, alongside the ability to compare ASVs among different studies, makes ASVs more practical than OTUs for functional gene analysis in environmental microbiology. Finally, we



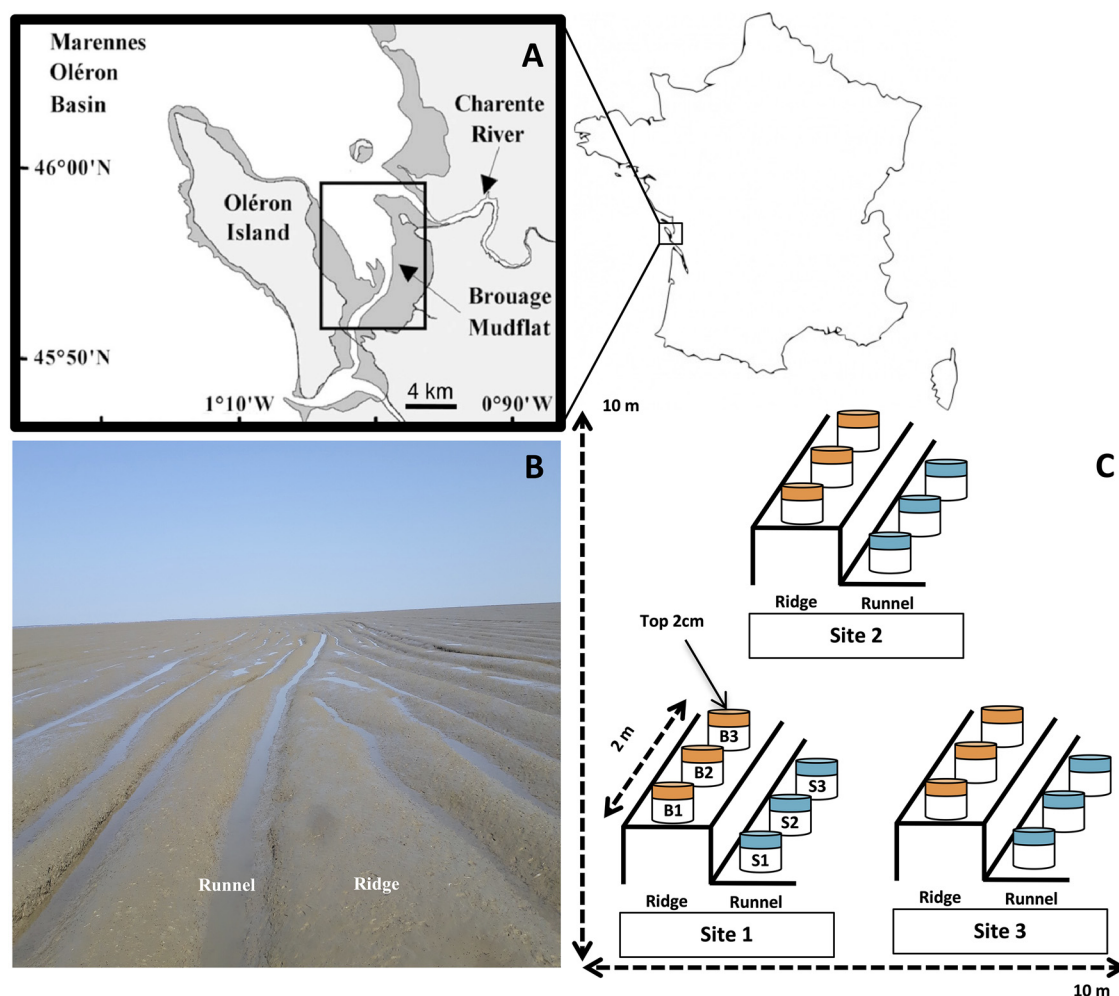


**FIG 7** Sediment sampling of ridges and runnels on the Brouage mudflat. (A) Map showing the location of the Brouage mudflat on the Marennes-Oléron Bay on the French Atlantic coast. (B) Parallel ridge-runnel sedimentary structures that characterize the intertidal mudflat. (C) Schematic of the sampling plan. Three ridges-runnels within  $\sim 25 \text{ m}^2$  were sampled. For each ridge-runnel structure, replicate ( $n = 3$ ) sediment cores (2-cm depth) were taken from the ridges and runnels along an  $\sim 2\text{-m}$  transect.

recommend the use of a relevant database that closely resembles the expected sequences from the environment studied along with the BLCA method for taxonomic classification. If such a database cannot be obtained, the NBC approach might yield better results.

## MATERIALS AND METHODS

**Similarity thresholds from the literature used to cluster OTUs for nitrogen cycle genes.** Similarity thresholds were selected based on a literature review for all amplicon-based nitrogen cycle studies. The list provided in Table 1 is, to the best of our knowledge, an exhaustive representation of OTU similarity thresholds used for the genes tested.

**Sample collection, physicochemical measurements, PCR, and Illumina sequencing.** Triplicate surface mud cores (0 to 2 cm) were sampled in July 2016 from the Montportail-Brouage mudflat, France, from three different ridges and runnels within  $27.41 \text{ m}^2$  (location 1 [L1],  $45^\circ 54' 31.50'' \text{ N}$ ,  $001^\circ 05' 14.60'' \text{ W}$ ; location 2 [L2],  $45^\circ 54' 31.70'' \text{ N}$ ,  $001^\circ 05' 14.20'' \text{ W}$ ; location 3 [L3],  $45^\circ 54' 31.50'' \text{ N}$ ,  $001^\circ 05' 14.20'' \text{ W}$ ) (57, 58) at the VASIREMI station (Fig. 7). Sediment was homogenized, collected in sterile 5-mL syringes, flash-frozen, and stored at  $-80^\circ \text{C}$  until subsequent use. Biophysicochemical parameters were measured as described previously (58); detailed procedures are provided in Text S1 in the supplemental material. DNA extraction was carried out using a modification of a protocol developed previously (59), and PCR of the *amoA* (bacteria and archaea), *nirB*, *nirSK*, and *nrfA* genes was carried out as detailed in Table 5. Illumina amplicon sequencing library preparation was carried out as described previously by Cholet et al. (10), using the Nextera XT index kit (Illumina, UK). Products were pooled at equimolar concentrations and submitted to the Earlham Institute (Norwich, UK) for Illumina MiSeq sequencing (300PE (Paired-End); 22 million reads/lane). Detailed protocols are provided in Text S1.

**TABLE 5** List of primers and corresponding PCR conditions used in this study

| Primer      | Sequence (5'–3')     | Orientation | Target   | Length (bp) | PCR conditions  | Reference |
|-------------|----------------------|-------------|--|-------------|---|-----------|
| BacamoA-1F  | GGGGHTTYTACTGGTGGT   | Forward     | <i>amoA</i> ; ammonia oxidation (bacteria)           | 491         | 95°C for 15 min; 32 cycles of 94°C for 30 s, 47°C for 40 s, and 72°C for 1 min; and 72°C for 10 min | 94        |
| BacamoA-2R  | CCCCTCBGSAAVCCCTCTTC | Reverse     |  |             |   |           |
| Arch-amoWAF | CTGAYTGGGCTGGACATC   | Forward     | <i>amoA</i> ; ammonia oxidation (archaea)            | 256         | 95°C for 15 min; 35 cycles of 95°C for 30 s, 58°C for 40 s, and 72°C for 1 min; and 72°C for 10 min | 95        |
| Arch-amoWAR | TTCTTCTTTGTGCCAGTA   | Reverse     |  |             |   |           |
| nirK FlaCu  | ATCATGGTCTGCCGCG     | Forward     | <i>nirK</i> ; nitrite reductase                      | 472         | 95°C for 15 min; 30 cycles of 95°C for 30 s, 57°C for 30 s, and 72°C for 40 s; and 72°C for 10 min  | 96        |
| nirK R3Cu   | GCCTCGATCAGRTTGTGGTT | Reverse     |  |             |   |           |
| nirS1F      | CCTAYTGGCCGGRCART    | Forward     | <i>nirS</i> ; nitrite reductase                      | 256         | 95°C for 15 min; 30 cycles of 95°C for 30 s, 57°C for 30 s, and 72°C for 40 s; and 72°C for 10 min  | 97        |
| nirS 3R     | GCCGCCGTCRTGVAGGAA   | Reverse     |  |             |   |           |
| nrfAF2aw    | CARTGYCAYGTBGARTA    | Forward     | <i>nrfA</i> ; nitrite reduction (DNRA)               | 250         | 95°C for 15 min; 35 cycles of 94°C for 30 s, 50°C for 20 s, and 72°C for 40 s; and 72°C for 10 min  | 98        |
| nrfAR1      | TWNGGCATRTGRCARTC    | Reverse     |  |             |   |           |
| nxB169f     | TACATGTGGTGAACA      | Forward     | <i>nxB</i> ; nitrite oxidation ( <i>Nitrospira</i> ) | 485         | 95°C for 15 min; 30 cycles of 94°C for 30 s, 56°C for 30 s, and 72°C for 1 min; and 72°C for 10 min | 99        |
| nxB638r     | CGGTCTTGGTCRATCA     | Reverse     |  |             |   |           |

**OTU and ASV construction.** To construct OTUs, paired-end reads were trimmed and filtered with Sickle v1.2 (60) using a sliding window and trimming regions where the average base quality was below 20. A 10-bp threshold was used to discard reads below this length. BayesHammer (60) and Spades v2.5.0 assembler were used to error correct paired-end reads, followed by pandaseq v2.4 with a minimum overlap of 20 bp to assemble the forward and reverse reads into a single sequence. The choice of software was a result of our recent work (61, 62) where it was shown that the above-described strategy of read trimming followed by error correction and overlapping reads reduces the substitution rates significantly. After having obtained the consensus sequences from each sample, the VSEARCH (v2.3.4) pipeline (all of these steps are documented at <https://github.com/torognes/vsearch/wiki/VSEARCH-pipeline>) was used for OTU construction. Reads were pooled from different samples, and barcodes were added to keep an account of the samples that the reads originated from. Reads were then dereplicated and sorted by decreasing abundance, and singletons were discarded. In the next step, the reads were clustered based on different similarity thresholds (97%, 95%, 90%, and 85% for AOA and AOB *amoA*; 97%, 95%, 90%, and 83% or 82% for *nirK* [83%] and *nirS* [82%]; and 97% for *nxB* and *nrfA*), followed by the removal of clusters that have chimeric models built from more abundant reads (–uchime\_denovo option in VSEARCH). A few chimeras may be missed, especially if they have parents that are absent from the reads or are present at a very low abundance. Therefore, in the next step, we used a reference-based chimera-filtering step (–uchime\_ref option in VSEARCH) using the reference databases created as described above. The quality-filtered barcoded reads were matched against clean OTUs with different similarity thresholds to generate OTU tables.

Amplicon sequence variants (ASVs) were constructed in R using the DADA2 package, according to the tutorial at <https://benjjneb.github.io/dada2/tutorial.html>. First, quality trimming was done using filterAndTrim(). The trimRight and trimLeft parameters, used to trim the 3' ends of reads and primer sequences, respectively, were adjusted for each target gene, as listed in Table S1. The 3'-end trimming length was adjusted to remove low-quality portions of the reads while still allowing a minimum of a 20-bp overlap between the forward and reverse reads, except for AOB *amoA* and *nxB*, where the minimum overlap was reduced to 4 bp. Error models were generated against the filtered forward and reverse reads using the learnErrors() function. Reads were then dereplicated using the derepFastq() function, and ASVs were inferred using the dada() function. Forward and reverse reads were merged using mergePairs(). A sequence table was generated using the makeSequenceTable() function, and chimeras were removed using the removeBimeraDenovo() function. A count table was then generated, and distances between the representative ASVs were inferred by aligning the sequences using Mafft (63) and constructing a phylogenetic tree using FastTree (64). The R script used for ASV construction is available in Text S1.

**Taxonomic assignment by NBC and BLCA.** For each nitrogen cycle gene, reference sequences (nucleotides) were downloaded from Fungene (<http://fungene.cme.msu.edu/>); for AOA and AOB *amoA*, a second database was constructed by downloading the sequences corresponding to the different clusters defined previously by Zhang et al. (8). Subsequently, the R rentrez package (65) was used to obtain taxonomic information at different levels, generating a taxonomy file. The FASTA file and the corresponding taxonomy file were formatted to work with Qiime (66).

To assign taxonomy to the representative ASVs, two different approaches were used: representative ASVs were classified using a naive Bayesian classifier (NBC) k-mer classifier (Qiime feature classifier classify-sklearn) or the Bayesian lowest common ancestor (BLCA) (39) against the reference databases, using default parameters. A detailed protocol for BLCA can be found at <https://github.com/qunfengdong/BLCA>. Count tables, generated in the previous step, and taxonomy tables were combined to generate biom files using Qiime (66) (<https://qiime2.org>) (biom add-metadata), and the phyloseq package was used to load these biom files in R.

**Amplicon read quality check.** After OTU and ASV construction, a quality check step was undertaken to ensure the reliability of the data. First, the correct reading frame was determined for OTU/ASV nucleotide sequences (from which primer sequences were removed) using the EXPASY translate online tool (<https://web.expasy.org/translate/>) and performing a BLAST search for the six different proteins against the standard non-redundant (nr) database using the BLASTp algorithm with default settings. All nucleotide sequences were then translated to protein sequences using the translate() function from the seqinr R package (67). The resulting amino acid (AA) sequences were separated into two categories: one containing AA sequences of the expected length (Table S2) and one containing AA sequences longer or shorter than the expected length. The latter sequences were submitted to a BLAST search against the standard nr database using the BLASTp algorithm. Sequences that matched the expected enzyme were then reintegrated into the first category of verified sequences. For downstream statistical analyses in R, abundance tables and phylogenetic trees were curated by retaining only these verified sequences.

**Downstream statistical analyses. (i) Alpha diversity indices.** The vegan package (68) was used to calculate richness (vegan::rarefy), Shannon entropy, and Simpson diversity (vegan::diversity) separately in ridges and runnels after rarefaction to 10,000 reads. Visualization was achieved using the ggplot2 package (<https://cran.r-project.org/web/packages/ggplot2/index.html>).

**(ii) Rarefaction curves.** Average abundance tables were generated by calculating the average abundance of each OTU/ASV in ridges and runnels. Rarefaction curves were then computed using the iNEXT package (69). Visualization was achieved using ggiNEXT().

**(iii) Beta diversity indices.** Abundance tables and phylogenetic trees were combined using phyloseq's merge\_phyloseq() function. Distances (Bray-Curtis/UniFrac/WUniFrac) between samples were calculated using phyloseq's phyloseq::distance() function and used for PERMANOVAs using vegan's adonis() function to determine if the sediment type (ridges and runnels) had a significant effect on the community composition. Visualization was achieved using the ggplot2 package (<https://cran.r-project.org/web/packages/ggplot2/index.html>).

**(iv) Mantel correlation tests.** Distances (Bray-Curtis/UniFrac/WUniFrac) between samples were calculated using phyloseq's phyloseq::distance() function, and the correlations between distance matrices were calculated using mantel.test() (nrepet = 9,999, "two-sided") from the ade4 package in R (<https://www.jstatsoft.org/article/view/v086i01>).

**(v) Canonical correspondence analysis.** To find significant drivers of the nitrogen-cycling communities, a canonical correspondence analysis (CCA) was carried out in R. First, the abundance tables (i.e., the OTU/ASV counts for each target in each sample) were normalized using the Hellinger transformation (70). Next, the parameter table (i.e., the table containing the biophysicochemical parameters for each sample) was normalized by centering and reduction. The CCA was then computed using the cca function from the R vegan package (68), with the standardized parameter table as the explanatory table and the Hellinger-transformed OTU/ASV abundance table as the response table. Variable selection was then carried out using the ordistep function (vegan package) with the option direction="both," allowing simultaneous backward and forward selection to find significant drivers for each target gene.

**(vi) Comparison of phylogenetic trees.** To evaluate the effects of HTS data processing methods on the phylogeny of representative sequences, representative sequences were aligned with closely related reference sequences obtained from the NCBI and/or Fungene database (for a list of reference sequences, see Table S3) using Mafft (63), and phylogenetic trees were generated using FastTree (64). In the first iteration, only the reference sequences and the most abundant ASVs/OTUs were included in the tree, and distances between trees were calculated using the Robinson-Foulds metric in R using the RF.dist() function from the Phangorn package (71). Additional ASVs/OTUs were added one by one in descending order of abundance. After each addition, the distances between trees were computed. Because the RF.dist() function requires equal numbers of tips in the trees compared, the total number of iterations corresponds to the number of sequences in the abundance table with the lowest number of sequences (e.g., for AOB *amoA*, there were 384 ASVs and 8 OTUs-85%; therefore, a maximum of 8 iterations were done when comparing AOB *amoA* ASV and OTU-85% trees).

**Data availability.** Raw reads were submitted to the NCBI database under accession number [PRJNA841793](https://www.ncbi.nlm.nih.gov/submit/PRJNA841793).

## SUPPLEMENTAL MATERIAL

Supplemental material is available online only.

**TEXT S1**, DOCX file, 0.04 MB.

**FIG S1**, PDF file, 0.3 MB.

**FIG S2**, PDF file, 0.8 MB.

**FIG S3**, PDF file, 0.05 MB.

**TABLE S1**, DOCX file, 0.01 MB.

**TABLE S2**, DOCX file, 0.01 MB.

**TABLE S3**, DOCX file, 0.02 MB.

**TABLE S4**, DOCX file, 0.02 MB.

## ACKNOWLEDGMENTS

We acknowledge the cytometry and imaging facilities and the molecular core facilities of the LIENSs laboratory, University of La Rochelle.

We acknowledge the following funders: Thomas Crawford Hayes NUIG (awarded to C.J.S. and A.L.), a Harry Smith vacation studentship (awarded to A.L.), a mobility grant from the French Embassy in Ireland (awarded to H.A. and C.J.S.), a research visit grant, a Microbiology Society and Research Student Mobility grant, the University of Glasgow (awarded to F.C.), La Rochelle University, and the Environmental Protection Agency STRIVE Doctoral Scholarship Scheme (2012-W-PhD-6) (awarded to C.J.S.). F.C. is supported by a University of Glasgow College of Science and Engineering doctoral scholarship, U.Z.I. was funded by NERC IRF NE/L011956/1, and C.J.S. is supported by a Royal Academy of Engineering-Scottish Water Research Chair (RCSR1718643) and EPSRC award EP/V030515/1.

## REFERENCES

- Shokralla S, Spall JL, Gibson JF, Hajibabaei M. 2012. Next-generation sequencing technologies for environmental DNA research. *Mol Ecol* 21: 1794–1805. <https://doi.org/10.1111/j.1365-294X.2012.05538.x>.
- Shendure J, Balasubramanian S, Church GM, Gilbert W, Rogers J, Schloss JA, Waterston RH. 2017. DNA sequencing at 40: past, present and future. *Nature* 550:345–353. <https://doi.org/10.1038/nature24286>.
- Roux S, Enault F, Bronner G, Debroas D. 2011. Comparison of 16S rRNA and protein-coding genes as molecular markers for assessing microbial diversity (Bacteria and Archaea) in ecosystems. *FEMS Microbiol Ecol* 78: 617–628. <https://doi.org/10.1111/j.1574-6941.2011.01190.x>.
- Poirier S, Rué O, Peguillan R, Coeuret G, Zagorec M, Champomier-Vergès MC, Loux V, Chaillou S. 2018. Deciphering intra-species bacterial diversity of meat and seafood spoilage microbiota using gyrB amplicon sequencing: a comparative analysis with 16S rDNA V3-V4 amplicon sequencing. *PLoS One* 13:e0204629. <https://doi.org/10.1371/journal.pone.0204629>.
- Sun DL, Jiang X, Wu QL, Zhou NY. 2013. Intragenomic heterogeneity of 16S rRNA genes causes overestimation of prokaryotic diversity. *Appl Environ Microbiol* 79:5962–5969. <https://doi.org/10.1128/AEM.01282-13>.
- Wu YC, Lu L, Wang BZ, Lin XG, Zhu JG, Cai ZC, Yan XY, Jia ZJ. 2011. Long-term field fertilization significantly alters community structure of ammonia-oxidizing bacteria rather than archaea in a paddy soil. *Soil Sci Soc Am J* 75:1431–1439. <https://doi.org/10.2136/sssaj2010.0434>.
- Duff AM, Zhang L-M, Smith CJ. 2017. Small-scale variation of ammonia oxidisers within intertidal sediments dominated by ammonia-oxidising bacteria *Nitrosomonas* sp. amoA genes and transcripts. *Sci Rep* 7:13200. <https://doi.org/10.1038/s41598-017-13583-x>.
- Zhang LM, Duff AM, Smith CJ. 2018. Community and functional shifts in ammonia oxidizers across terrestrial and marine (soil/sediment) boundaries in two coastal bay ecosystems. *Environ Microbiol* 20:2834–2853. <https://doi.org/10.1111/1462-2920.14238>.
- Aigle A, Prosser JI, Gubry-Rangin C. 2019. The application of high-throughput sequencing technology to analysis of amoA phylogeny and environmental niche specialisation of terrestrial bacterial ammonia-oxidisers. *Environ Microbiome* 14:3. <https://doi.org/10.1186/s40793-019-0342-6>.
- Cholet F, Ijaz UZ, Smith CJ. 2019. Differential ratio amplicons (R amp) for the evaluation of RNA integrity extracted from complex environmental samples. *Environ Microbiol* 21:827–844. <https://doi.org/10.1111/1462-2920.14516>.
- Cholet F, Ijaz UZ, Smith CJ. 2020. Reverse transcriptase enzyme and priming strategy affect quantification and diversity of environmental transcripts. *Environ Microbiol* 22:2383–2402. <https://doi.org/10.1111/1462-2920.15017>.
- Zhang Y, Wang X, Zhen Y, Mi T, He H, Yu Z. 2017. Microbial diversity and community structure of sulfate-reducing and sulfur-oxidizing bacteria in sediment cores from the East China Sea. *Front Microbiol* 8:2133. <https://doi.org/10.3389/fmicb.2017.02133>.
- Marshall IPG, Ren G, Jaussi M, Lomstein BA, Jørgensen BB, Røy H, Kjeldsen KU. 2019. Environmental filtering determines family-level structure of sulfate-reducing microbial communities in subsurface marine sediments. *ISME J* 13:1920–1932. <https://doi.org/10.1038/s41396-019-0387-y>.
- Dziewit L, Pyzik A, Romaniuk K, Sobczak A, Szczesny P, Lipinski L, Bartosik D, Drewniak L. 2015. Novel molecular markers for the detection of methanogens and phylogenetic analyses of methanogenic communities. *Front Microbiol* 6:694. <https://doi.org/10.3389/fmicb.2015.00694>.
- Varjian SJ, Upasani VN. 2017. A new look on factors affecting microbial degradation of petroleum hydrocarbon pollutants. *Int Biodeterior Biodegradation* 120:71–83. <https://doi.org/10.1016/j.ibiod.2017.02.006>.
- Liu LY, Xie GJ, Xing DF, Liu BF, Ding J, Cao GL, Ren NQ. 2021. Sulfate dependent ammonium oxidation: a microbial process linked nitrogen with sulfur cycle and potential application. *Environ Res* 192:110282. <https://doi.org/10.1016/j.envres.2020.110282>.
- Fournier PE, Dubourg G, Raoult D. 2014. Clinical detection and characterization of bacterial pathogens in the genomics era. *Genome Med* 6:114–115. <https://doi.org/10.1186/s13073-014-0114-2>.
- Edgar RC. 2018. Updating the 97% identity threshold for 16S ribosomal RNA OTUs. *Bioinformatics* 34:2371–2375. <https://doi.org/10.1093/bioinformatics/bty113>.
- Green J, Bohannan BJM. 2006. Spatial scaling of microbial biodiversity. *Trends Ecol Evol* 21:501–507. <https://doi.org/10.1016/j.tree.2006.06.012>.
- Horner-Devine MC, Lage M, Hughes JB, Bohannan BJM. 2004. A taxa-area relationship for bacteria. *Nature* 432:750–753. <https://doi.org/10.1038/nature03073>.
- Storch D, Szilang AL. 2008. The concept of taxon invariance in ecology: do diversity patterns vary with changes in taxonomic resolution? *Folia Geobot* 43:329–344. <https://doi.org/10.1007/s12224-008-9015-8>.
- Chen W, Zhang CK, Cheng Y, Zhang S, Zhao H. 2013. A comparison of methods for clustering 16S rRNA sequences into OTUs. *PLoS One* 8: e70837. <https://doi.org/10.1371/journal.pone.0070837>.
- Brown EA, Chain FJJ, Crease TJ, Macisaac HJ, Cristescu ME. 2015. Divergence thresholds and divergent biodiversity estimates: can metabarcoding reliably describe zooplankton communities? *Ecol Evol* 5:2234–2251. <https://doi.org/10.1002/ece3.1485>.
- Koepfel AF, Wu M. 2013. Surprisingly extensive mixed phylogenetic and ecological signals among bacterial operational taxonomic units. *Nucleic Acids Res* 41:5175–5188. <https://doi.org/10.1093/nar/gkt241>.
- Schmidt TSB, Matias Rodrigues JF, von Mering C. 2015. Limits to robustness and reproducibility in the demarcation of operational taxonomic units. *Environ Microbiol* 17:1689–1706. <https://doi.org/10.1111/1462-2920.12610>.
- Callahan BJ, McMurdie PJ, Holmes SP. 2017. Exact sequence variants should replace operational taxonomic units in marker-gene data analysis. *ISME J* 11:2639–2643. <https://doi.org/10.1038/ismej.2017.119>.
- Edgar RC. 2017. Accuracy of microbial community diversity estimated by closed- and open-reference OTUs. *PeerJ* 5:e3889. <https://doi.org/10.7717/peerj.3889>.
- Callahan BJ, McMurdie PJ, Rosen MJ, Han AW, Johnson AJA, Holmes SP. 2016. DADA2: high-resolution sample inference from Illumina amplicon data. *Nat Methods* 13:581–583. <https://doi.org/10.1038/nmeth.3869>.
- Amir A, McDonald D, Navas-Molina JA, Kopylova E, Morton JT, Zech Xu Z, Kightley EP, Thompson LR, Hyde ER, Gonzalez A, Knight R. 2017. Deblur rapidly resolves single-nucleotide community sequence patterns. *mSystems* 2:e00191-16. <https://doi.org/10.1128/mSystems.00191-16>.
- Nearing JT, Douglas GM, Comeau AM, Langille MGI. 2018. Denoising the denoisers: an independent evaluation of microbiome sequence error-correction approaches. *PeerJ* 6:e5364. <https://doi.org/10.7717/peerj.5364>.
- Caruso V, Song X, Asquith M, Karstens L. 2019. Performance of microbiome sequence inference methods in environments with varying biomass. *mSystems* 4:e00163-18. <https://doi.org/10.1128/mSystems.00163-18>.
- Moossavi S, Atakora F, Fehr K, Khafipour E. 2020. Biological observations in microbiota analysis are robust to the choice of 16S rRNA gene sequencing processing algorithm: case study on human milk microbiota. *BMC Microbiol* 20:290. <https://doi.org/10.1186/s12866-020-01949-7>.
- Pauvert C, Buée M, Laval V, Edel-Hermann V, Fauchery L, Gautier A, Lesur I, Vallance J, Vacher C. 2019. Bioinformatics matters: the accuracy of plant and soil fungal community data is highly dependent on the metabarcoding pipeline. *Fungal Ecol* 41:23–33. <https://doi.org/10.1016/j.funeco.2019.03.005>.
- Prodan A, Tremaroli V, Brolin H, Zwinderman AH, Nieuwdorp M, Levin E. 2020. Comparing bioinformatic pipelines for microbial 16S rRNA amplicon sequencing. *PLoS One* 15:e0227434. <https://doi.org/10.1371/journal.pone.0227434>.



35. Glassman SI, Martiny JHB. 2018. Broad-scale ecological patterns are robust to use of exact sequence variants versus operational taxonomic units. *mSphere* 3:e00148-18. <https://doi.org/10.1128/mSphere.00148-18>.
36. Joos L, Beirinckx S, Haegeman A, Debode J, Vandecasteele B, Baeyen S, Goormachtig S, Clement L, De Tender C. 2020. Daring to be differential: metabarcoding analysis of soil and plant-related microbial communities using amplicon sequence variants and operational taxonomic units. *BMC Genomics* 21:733. <https://doi.org/10.1186/s12864-020-07126-4>.
37. Wang Q, Garrity GM, Tiedje JM, Cole JR. 2007. Naïve Bayesian classifier for rapid assignment of rRNA sequences into the new bacterial taxonomy. *Appl Environ Microbiol* 73:5261–5267. <https://doi.org/10.1128/AEM.00062-07>.
38. Vinje H, Liland KH, Almøy T, Snipen L. 2015. Comparing K-mer based methods for improved classification of 16S sequences. *BMC Bioinformatics* 16:205. <https://doi.org/10.1186/s12859-015-0647-4>.
39. Gao X, Lin H, Revanna K, Dong Q. 2017. A Bayesian taxonomic classification method for 16S rRNA gene sequences with improved species-level accuracy. *BMC Bioinformatics* 18:247. <https://doi.org/10.1186/s12859-017-1670-4>.
40. Thom C, Smith CJ, Moore G, Weir P, Ijaz UZ. 2022. Microbiomes in drinking water treatment and distribution: a meta-analysis from source to tap. *Water Res* 212:118106. <https://doi.org/10.1016/j.watres.2022.118106>.
41. Laima M, Brossard D, Sauriau P-G, Girard M, Richard P, Goulet D, Joassard L. 2002. The influence of long emersion on biota, ammonium fluxes and nitrification in intertidal sediments of Marennes-Oléron Bay, France. *Mar Environ Res* 53:381–402. [https://doi.org/10.1016/S0141-1136\(01\)00126-X](https://doi.org/10.1016/S0141-1136(01)00126-X).
42. Laima MJC, Girard MF, Vouvé F, Richard P, Blanchard G, Goulet D. 1999. Nitrification rates related to sedimentary structures in an Atlantic intertidal mudflat, Marennes-Oleron Bay, France. *Mar Ecol Prog Ser* 191:33–41. <https://doi.org/10.3354/meps191033>.
43. Mohsen A, Park J, Chen Y-A, Kawashima H, Mizuguchi K. 2019. Impact of quality trimming on the efficiency of reads joining and diversity analysis of Illumina paired-end reads in the context of QIIME1 and QIIME2 microbiome analysis frameworks. *BMC Bioinformatics* 20:581. <https://doi.org/10.1186/s12859-019-3187-5>.
44. Prosser JL, Nicol GW. 2012. Archaeal and bacterial ammonia-oxidisers in soil: the quest for niche specialisation and differentiation. *Trends Microbiol* 20:523–531. <https://doi.org/10.1016/j.tim.2012.08.001>.
45. Ke X, Angel R, Lu Y, Conrad R. 2013. Niche differentiation of ammonia oxidizers and nitrite oxidizers in rice paddy soil. *Environ Microbiol* 15:2275–2292. <https://doi.org/10.1111/1462-2920.12098>.
46. Shen JP, Xu Z, He JZ. 2014. Frontiers in the microbial processes of ammonia oxidation in soils and sediments. *J Soils Sediments* 14:1023–1029. <https://doi.org/10.1007/s11368-014-0872-x>.
47. Gao D, Liu F, Xie Y, Liang H. 2018. Temporal and spatial distribution of ammonia-oxidizing organisms of two types of wetlands in Northeast China. *Appl Microbiol Biotechnol* 102:7195–7205. <https://doi.org/10.1007/s00253-018-9152-9>.
48. Hink L, Gubry-Rangin C, Nicol GW, Prosser JL. 2018. The consequences of niche and physiological differentiation of archaeal and bacterial ammonia oxidisers for nitrous oxide emissions. *ISME J* 12:1084–1093. <https://doi.org/10.1038/s41396-017-0025-5>.
49. Hou L, Xie X, Wan X, Kao S-J, Jiao N, Zhang Y. 2018. Niche differentiation of ammonia and nitrite oxidizers along a salinity gradient from the Pearl River estuary to the South China Sea. *Biogeosciences* 15:5169–5187. <https://doi.org/10.5194/bg-15-5169-2018>.
50. Aigle A, Gubry-Rangin C, Thion C, Estera-Molina KY, Richmond H, Pett-Ridge J, Firestone MK, Nicol GW, Prosser JL. 2020. Experimental testing of hypotheses for temperature- and pH-based niche specialization of ammonia oxidizing archaea and bacteria. *Environ Microbiol* 22:4032–4045. <https://doi.org/10.1111/1462-2920.15192>.
51. Jia Z, Zhou X, Xia W, Fornara D, Wang B, Wasson EA, Christie P, Polz MF, Myrold DD. 2020. Evidence for niche differentiation of nitrifying communities in grassland soils after 44 years of different field fertilization scenarios. *Pedosphere* 30:87–97. [https://doi.org/10.1016/S1002-0160\(19\)60803-9](https://doi.org/10.1016/S1002-0160(19)60803-9).
52. García-López R, Cornejo-Granados F, Lopez-Zavala AA, Cota-Huizar A, Sotelo-Mundo RR, Gómez-Gil B, Ochoa-Leyva A. 2021. OTUs and ASVs produce comparable taxonomic and diversity using tailored abundance filters. *Genes (Basel)* 12:564. <https://doi.org/10.3390/genes12040564>.
53. Schloss PD. 2021. Amplicon sequence variants artificially split bacterial genomes into separate clusters. *mSphere* 6:e00191-21. <https://doi.org/10.1128/mSphere.00191-21>.
54. García-García N, Tamames J, Linz AM, Pedrós-Alió C, Puente-Sánchez F. 2019. Microdiversity ensures the maintenance of functional microbial communities under changing environmental conditions. *ISME J* 13:2969–2983. <https://doi.org/10.1038/s41396-019-0487-8>.
55. Chain P, Lamerdin J, Larimer F, Regala W, Lao V, Land M, Hauser L, Alan H, Klotz M, Norton J, Sayavedra-Soto L, Arciero D, Hommes N, Whittaker M, Arp D. 2003. Complete genome sequence of the ammonia-oxidizing bacterium and obligate chemolithoautotroph *Nitrosomonas europaea*. *J Bacteriol* 185:2759–2773. <https://doi.org/10.1128/JB.185.9.2759-2773.2003>.
56. Norton JM, Klotz MG, Stein LY, Arp DJ, Bottomley PJ, Chain PSG, Hauser LJ, Land ML, Larimer FW, Shin MW, Starkenburg SR. 2008. Complete genome sequence of *Nitrosospora multiformis*, an ammonia-oxidizing bacterium from the soil environment. *Appl Environ Microbiol* 74:3559–3572. <https://doi.org/10.1128/AEM.02722-07>.
57. Agogue H, Mallet C, Orvain F, De Crignis M, Mornet F, Dupuy C. 2014. Bacterial dynamics in a microphytobenthic biofilm: a tidal mesocosm approach. *J Sea Res* 92:36–45. <https://doi.org/10.1016/j.seares.2014.03.003>.
58. Laverne C, Agogue H, Leynaert A, Raimonet M, De Wit R, Pineau P, Bréret M, Lachaussee N, Dupuy C. 2017. Factors influencing prokaryotes in an intertidal mudflat and the resulting depth gradients. *Estuar Coast Shelf Sci* 189:74–83. <https://doi.org/10.1016/j.ecss.2017.03.008>.
59. Griffiths RI, Whiteley AS, O'Donnell AG, Bailey MJ. 2000. Rapid method for coextraction of DNA and RNA from natural environments for analysis of ribosomal DNA- and rRNA-based microbial community composition. *Appl Environ Microbiol* 66:5488–5491. <https://doi.org/10.1128/AEM.66.12.5488-5491.2000>.
60. Joshi NA, Fass JN. 2011. Sickle: a sliding-window, adaptive, quality-based trimming tool for FastQ files. <https://doi.org/10.1093/bioinformatics/btt053>.
61. Schirmer M, Ijaz UZ, D'Amore R, Hall N, Sloan WT, Quince C. 2015. Insight into biases and sequencing errors for amplicon sequencing with the Illumina MiSeq platform. *Nucleic Acids Res* 43:e37. <https://doi.org/10.1093/nar/gku1341>.
62. D'Amore R, Ijaz UZ, Schirmer M, Kenny JG, Gregory R, Darby AC, Shakya M, Podar M, Quince C, Hall N. 2016. A comprehensive benchmarking study of protocols and sequencing platforms for 16S rRNA community profiling. *BMC Genomics* 17:55. <https://doi.org/10.1186/s12864-015-2194-9>.
63. Katoh K, Asimenos G, Toh H. 2009. Multiple alignment of DNA sequences with MAFFT. *Methods Mol Biol* 537:39–64. [https://doi.org/10.1007/978-1-59745-251-9\\_3](https://doi.org/10.1007/978-1-59745-251-9_3).
64. Price MN, Dehal PS, Arkin AP. 2010. FastTree 2—approximately maximum-likelihood trees for large alignments. *PLoS One* 5:e9490. <https://doi.org/10.1371/journal.pone.0009490>.
65. Winter DJ. 2017. rentrez: an R package for the NCBI eUtils API. *R J* 9:520–526. <https://doi.org/10.32614/RJ-2017-058>.
66. Caporaso JG, Kuczynski J, Stombaugh J, Bittinger K, Bushman FD, Costello EK, Fierer N, Peña AG, Goodrich JK, Gordon JI, Huttenhower G, Kelley ST, Knights D, Koenig JE, Ley RE, Lozupone CA, McDonald D, Muegge BD, Pirrung M, Reeder J, Sevinsky JR, Turnbaugh PJ, Walters WA, Widmann J, Yatsunenko T, Zaneveld J, Knight R. 2010. QIIME allows analysis of high-throughput community sequencing data. *Nat Methods* 7:335–336. <https://doi.org/10.1038/nmethf.303>.
67. Charif D, Lobry JR. 2007. SeqinR 1.0-2: a contributed package to the R project for statistical computing devoted to biological sequences retrieval and analysis, p 207–232. *In* Bastolla U, Porto M, Roman HE, Vendruscolo M (ed), Structural approaches to sequence evolution: molecules, networks, populations. Springer, Berlin, Germany.
68. Oksanen J, Kindt R, O'Hara RB. 2005. vegan: community ecology package. <https://cran.r-project.org/web/packages/vegan/vegan.pdf>.
69. Hsieh TC, Ma KH, Chao A. 2016. iNEXT: an R package for rarefaction and extrapolation of species diversity (Hill numbers). *Methods Ecol Evol* 7: 1451–1456. <https://doi.org/10.1111/2041-210X.12613>.
70. Legendre P, Gallagher ED. 2001. Ecologically meaningful transformations for ordination of species data. *Oecologia* 129:271–280. <https://doi.org/10.1007/s004420100716>.
71. Schliep KP. 2011. phangorn: phylogenetic analysis in R. *Bioinformatics* 27: 592–593. <https://doi.org/10.1093/bioinformatics/btq706>.
72. Liu Y, Zhou H, Wang J, Liu X, Cheng K, Li L, Zheng J, Zhang X, Zheng J, Pan G. 2015. Short-term response of nitrifier communities and potential nitrification activity to elevated CO<sub>2</sub> and temperature interaction in a Chinese paddy field. *Appl Soil Ecol* 96:88–98. <https://doi.org/10.1016/j.apsoil.2015.06.006>.
73. Fang Y, Wang F, Jia X, Chen J. 2019. Distinct responses of ammonia-oxidizing bacteria and archaea to green manure combined with reduced chemical fertilizer in a paddy soil. *J Soils Sediments* 19:1613–1623. <https://doi.org/10.1007/s11368-018-2154-5>.
74. Nair RR, Boobal R, Vrinda S, Bright Singh IS, Valsamma J. 2019. Ammonia-oxidizing bacterial and archaeal communities in tropical bioaugmented zero water exchange shrimp production systems. *J Soils Sediments* 19: 2126–2142. <https://doi.org/10.1007/s11368-018-2185-y>.
75. Baskaran V, Patil PK, Antony ML, Avunje S, Nagaraju VT, Ghate SD, Nathamuni S, Dineshkumar N, Alavandi SV, Vijayan KK. 2020. Microbial community profiling

- of ammonia and nitrite oxidizing bacterial enrichments from brackishwater ecosystems for mitigating nitrogen species. *Sci Rep* 10:5201. <https://doi.org/10.1038/s41598-020-62183-9>.
76. Xia W, Zhang C, Zeng X, Feng Y, Weng J, Lin X, Zhu J, Xiong Z, Xu J, Cai Z, Jia Z. 2011. Autotrophic growth of nitrifying community in an agricultural soil. *ISME J* 5:1226–1236. <https://doi.org/10.1038/ismej.2011.5>.
  77. Mosier AC, Francis CA. 2008. Relative abundance and diversity of ammonia-oxidizing archaea and bacteria in the San Francisco Bay estuary. *Environ Microbiol* 10:3002–3016. <https://doi.org/10.1111/j.1462-2920.2008.01764.x>.
  78. Peng X, Yando E, Hildebrand E, Dwyer C, Kearney A, Waciga A, Valiela I, Bernhard AE. 2013. Differential responses of ammonia-oxidizing archaea and bacteria to long-term fertilization in a New England salt marsh. *Front Microbiol* 3:445. <https://doi.org/10.3389/fmicb.2012.00445>.
  79. Smith JM, Mosier AC, Francis CA. 2015. Spatiotemporal relationships between the abundance, distribution, and potential activities of ammonia-oxidizing and denitrifying microorganisms in intertidal sediments. *Microb Ecol* 69:13–24. <https://doi.org/10.1007/s00248-014-0450-1>.
  80. Sun R, Myrold DD, Wang D, Guo X, Chu H. 2019. AOA and AOB communities respond differently to changes of soil pH under long-term fertilization. *Soil Ecol Lett* 1:126–135. <https://doi.org/10.1007/s42832-019-0016-8>.
  81. Abell GCJ, Banks J, Ross DJ, Keane JP, Robert SS, Revill AT, Volkman JK. 2011. Effects of estuarine sediment hypoxia on nitrogen fluxes and ammonia oxidizer gene transcription. *FEMS Microbiol Ecol* 75:111–122. <https://doi.org/10.1111/j.1574-6941.2010.00988.x>.
  82. Baolan H, Shuai L, Lidong S, Ping Z, Xiangyang X, Liping L. 2012. Effect of different ammonia concentrations on community succession of ammonia-oxidizing microorganisms in a simulated paddy soil column. *PLoS One* 7:e44122. <https://doi.org/10.1371/journal.pone.0044122>.
  83. Pester M, Rattei T, Flechl S, Gröngroft A, Richter A, Overmann J, Reinhold-Hurek B, Loy A, Wagner M. 2012. AmoA-based consensus phylogeny of ammonia-oxidizing archaea and deep sequencing of amoA genes from soils of four different geographic regions. *Environ Microbiol* 14:525–539. <https://doi.org/10.1111/j.1462-2920.2011.02666.x>.
  84. Stempfhuber B, Richter-Heitmann T, Regan KM, Kölbl A, Wüst PK, Marhan S, Sikorski J, Overmann J, Friedrich MW, Kandeler E, Schlöter M. 2016. Spatial interaction of archaeal ammonia-oxidizers and nitrite-oxidizing bacteria in an unfertilized grassland soil. *Front Microbiol* 6:1567. <https://doi.org/10.3389/fmicb.2015.01567>.
  85. Biller SJ, Mosier AC, Wells GF, Francis CA. 2012. Global biodiversity of aquatic ammonia-oxidizing archaea is partitioned by habitat. *Front Microbiol* 3:252. <https://doi.org/10.3389/fmicb.2012.00252>.
  86. Lund MB, Smith JM, Francis CA. 2012. Diversity, abundance and expression of nitrite reductase (nirK)-like genes in marine thaumarchaea. *ISME J* 6:1966–1977. <https://doi.org/10.1038/ismej.2012.40>.
  87. Wei W, Isobe K, Nishizawa T, Zhu L, Shiratori Y, Ohte N, Koba K, Otsuka S, Senoo K. 2015. Higher diversity and abundance of denitrifying microorganisms in environments than considered previously. *ISME J* 9:1954–1965. <https://doi.org/10.1038/ismej.2015.9>.
  88. Shi R, Xu S, Qi Z, Huang H, Liang Q. 2019. Seasonal patterns and environmental drivers of nirS- and nirK-encoding denitrifiers in sediments of Daya Bay, China. *Oceanologia* 61:308–320. <https://doi.org/10.1016/j.oceano.2019.01.002>.
  89. Aalto SL, Saarenheimo J, Arvola L, Tirola M, Huotari J, Rissanen AJ. 2019. Denitrifying microbial communities along a boreal stream with varying land-use. *Aquat Sci* 81:59. <https://doi.org/10.1007/s00027-019-0654-z>.
  90. Thompson KA, Bent E, Abalos D, Wagner-Riddle C, Dunfield KE. 2016. Soil microbial communities as potential regulators of in situ N<sub>2</sub>O fluxes in annual and perennial cropping systems. *Soil Biol Biochem* 103:262–273. <https://doi.org/10.1016/j.soilbio.2016.08.030>.
  91. Papaspyrou S, Smith CJ, Dong LF, Whitby C, Dumbrell AJ, Nedwell DB. 2014. Nitrate reduction functional genes and nitrate reduction potentials persist in deeper estuarine sediments. Why? *PLoS One* 9:e94111. <https://doi.org/10.1371/journal.pone.0094111>.
  92. Bu C, Wang Y, Ge C, Ahmad HA, Gao B, Ni S-Q. 2017. Dissimilatory nitrate reduction to ammonium in the Yellow River Estuary: rates, abundance, and community diversity. *Sci Rep* 7:6830. <https://doi.org/10.1038/s41598-017-06404-8>.
  93. Ramanathan B, Boddicker AM, Roane TM, Mosier AC. 2017. Nitrifier gene abundance and diversity in sediments impacted by acid mine drainage. *Front Microbiol* 8:2136. <https://doi.org/10.3389/fmicb.2017.02136>.
  94. Hornek R, Pommerening-Röser A, Koops HP, Farnleitner AH, Kreuzinger N, Kirschner A, Mach RL. 2006. Primers containing universal bases reduce multiple amoA gene specific DGGE band patterns when analysing the diversity of beta-ammonia oxidizers in the environment. *J Microbiol Methods* 66:147–155. <https://doi.org/10.1016/j.mimet.2005.11.001>.
  95. Wuchter C, Abbas B, Coolen MJL, Herfort L, van Bleijswijk J, Timmers P, Strous M, Teira E, Herndl GJ, Middelburg JJ, Schouten S, Sinninghe Damsté JS. 2006. Archaeal nitrification in the ocean. *Proc Natl Acad Sci U S A* 103:12317–12322. <https://doi.org/10.1073/pnas.0600756103>.
  96. Hallin S, Lindgren PE. 1999. PCR detection of genes encoding nitrite reductase in denitrifying bacteria. *Appl Environ Microbiol* 65:1652–1657. <https://doi.org/10.1128/AEM.65.4.1652-1657.1999>.
  97. Levy-Booth DJ, Prescott CE, Grayston SJ. 2014. Microbial functional genes involved in nitrogen fixation, nitrification and denitrification in forest ecosystems. *Soil Biol Biochem* 75:11–25. <https://doi.org/10.1016/j.soilbio.2014.03.021>.
  98. Welsh A, Chee-Sanford JC, Connor LM, Löffler FE, Sanford RA. 2014. Refined nrfA phylogeny improves PCR-based nrfA gene detection. *Appl Environ Microbiol* 80:2110–2119. <https://doi.org/10.1128/AEM.03443-13>.
  99. Pester M, Maixner F, Berry D, Rattei T, Koch H, Lückner S, Nowka B, Richter A, Spieck E, Lebedeva E, Loy A, Wagner M, Daims H. 2014. NxrB encoding the beta subunit of nitrite oxidoreductase as functional and phylogenetic marker for nitrite-oxidizing Nitrospira. *Environ Microbiol* 16:3055–3071. <https://doi.org/10.1111/1462-2920.12300>.